AN INVESTIGATION OF ACOUSTIC PHASE-SHIFT NETWORKS IN THE DESIGN OF UNIDIRECTIONAL, UNDERWATER SOUND TRANSDUCERS

By R. D. Marciniak

Technical Memorandum
File No. TM 409.3381-16
January 22, 1969
Contract NOw 65-0123-d
Copy No. 15

The Pennsylvania State University
Institute for Science and Engineering
ORDNANCE RESEARCH LABORATORY
University Park, Pennsylvania

NAVY DEPARTMENT · NAVAL ORDNANCE SYSTEMS COMMAND

ABSTRACT

A low-frequency, underwater sound transducer model was developed which utilized a liquid-filled, acoustic phase-shift network to obtain a unidirectional (cardioid) directivity response over a prescribed frequency range.

A number of analytical relationships between certain physical parameters of the device, its environment, and the acoustic phase shift network were studied to determine just how they should interact for the transducer to function as specified. A search was directed at finding and choosing an inert fluid (in this case a Dow Corning '200', 200 centistoke, silicone oil) which would satisfy the required acoustic phase-shift network parameters and also be relatively insensitive to a change in pressure (hence depth) and temperature. A study of the transducer design was carried out and a trilaminar, piezoceramic pressure-gradient element was selected in the final design of the model.

When the completed transducer model was configured as specified, a unidirectional (cardioid) response was achieved consistently between 4000 Hz and 6000 Hz. Front-to-back discriminations ranging between 15 dB and 22 dB were recorded over the upper half of the frequency range (5000 Hz to 6000 Hz), while 10 dB to 15 dB discriminations were recorded over the lower half (4000 Hz to 5000 Hz) of the frequency range. In addition, a nominally flat free-field voltage response (M_o) of -85 dB + 2 dB reference 1 V/ubar was achieved over the frequency range of 4000 Hz to 6000 Hz.

TABLE OF CONTENTS

TABLE OF CONTENTS

LIST OF FIGURES

LIST OF FIGURES

LIST OF TABLES

CHAPTER I

INTRODUCTION

1.1 General Discussion

Several methods exist by which combinations of pressure and pressure gradient air microphones have been employed to provide a unidirectional, (cardioid) directivity response at low frequencies. The invention of the ribbon (pressure gradient) microphone by Olson[1] undoubtedly provided the necessary breakthrough for the creation of one version of this type of unidirectional air microphone.[2,3] This earliest version combined the output of a pressure gradient microphone (in this case, a ribbon, freely accessible to the sound field on both sides) with a pressure microphone (another ribbon open to the sound field on the front side and terminated on the back side by a damped pipe).

The directional response of the pressure gradient element can be expressed by $R = \cos\theta$ (bidirectional) and that of the pressure element by $R = 1$ (omnidirectional), θ being the angle of incidence. Since the two lobes of the pressure gradient hydrophone have exactly opposite phases, the result of adding the output of the pressure element to that of the pressure gradient element is to just cancel the output in one direction on the axis and double it in the other with intermediate values in between. Hence, the resulting response is $R = (1 + \cos\theta)$. The same principle was used by Bauer[4] to obtain

a unidirectional response, except that he combined the output of a piezoelectric pressure gradient microphone with a piezoelectric pressure microphone to accomplish the task.

However, in 1938, Bauer[5,6,7] formulated an entirely different method to accomplish the same unidirectional objective. He used a single pressure gradient microphone with an "acoustic phase-shift network" to obtain the unidirectional response. A number of basic acoustic relations evolved from this work. That is, interrelationships between a number of acoustic impedance parameters and operating medium parameters, which are necessary to achieve the required phase shift, were derived. These relations are fairly easily satisfied for the air microphone. However, the task is not as readily accomplished for a device that must operate in a liquid (water) medium since this medium imposes entirely different physical constants and constraints.

1.2 Specific Definition of the Problem

The specific objective of this investigation is to develop a low frequency, underwater transducer model which will achieve the desired relationships with a unidirectional, (cardioid) pressure gradient transducer. Since the model is to be utilized in an underwater environment, it should be, over a required frequency range, insensitive to a change in depth and insensitive to a change in temperature. Therefore, a liquid-filled, acoustic phase-shifted, trilaminar pressure gradient element system will be studied to

determine if it can meet the requirements. A model of the device, after all analytical and design work has been completed, will be constructed to demonstrate the feasibility of the idea.

1.3 Glossary of Terms

A	linear delay network coefficient
B	linear delay network coefficient
C_A	acoustic compliance - cm^5/dyne
c	velocity of sound in fresh water - cm/sec
c_f	velocity of sound in fluid - cm/sec
d	front to back distance - cm
f	frequency - Hz
i_θ	current out of linear delay network - amperes
ℓ	slot length (parallel to the direction of fluid motion) - cm
M_A	acoustic inertance - grams/cm^4
M_o	free field voltage response - dB reference 1 V/μbar
M_r	radiation mass - grams
m_{CONE}	mass rear cone - grams
N	linear delay network
P_n	acoustic pressure - dynes/cm^2
R	directional polar response
R_A	acoustic resistance - dynes-sec/cm^5
R_r	radiation resistance - grams/sec
S	effective radiating area - cm^2

t	slot thickness - cm
u_n	volume velocity - cm^3/sec
V	volume of the rear cavity - cm^3
W	slot width (perpendicular to the direction of fluid motion) - cm
X_θ	acoustic output of the theoretical model
X'_θ	acoustic output of the theoretical model
Z_A	acoustic impedance - dyne-sec/cm^5
β_f	adiabatic bulk modulus of the working fluid - dyne/cm^2
θ	angle of incidence - degrees
λ	wavelength of sound - cm
μ_f	dynamic viscosity of the fluid - dyne-sec/cm^2
ρ_f	density of fluid - grams/cm^3
φ	phase angle - radians
ω	radial frequency - radians/sec

CHAPTER I.

THEORETICAL CONSIDERATIONS

2.1 Development of a Theoretical Model

The following portion of this investigation was primarily aimed at putting together a complete and concise theoretical model from which a practical design of a single unit, pressure gradient, unidirectional, underwater sound transducer could be obtained.

Consider, as a first step in the development of the model, a device or a mechanism as presented in Figure 2.1. Allow the whole device enclosed within the dashed line to be irradiated by plane sound waves, incident at any angle θ, varying from 0° to ±180°. Let acoustic responsive elements be fixed at x and x', and, further, let them be displaced from each other by the distance d. The outputs of the acoustic elements X_θ and X'_θ, which are a result of the sound wave radiation, are then transferred to the linear delay network N. The current i_θ, which is the output of the delay network, will then flow through an output impedance Z. Recalling that the network is linear, it can be seen that

$$i_\theta = AX_\theta - BX'_\theta \quad , \tag{2.1}$$

or

$$i_\theta = A(X_\theta - \frac{B}{A} X'_\theta) \quad , \tag{2.2}$$

where A and B are the linear network coefficients which involve the elements of the linear delay network. Now, the current through the output impedance Z for sound arriving from the rear

of the device must be equal to zero if a unidirectional cardioid response is to be achieved. That is,

$$i_{180°} = 0 \quad . \tag{2.3}$$

Therefore, applying this condition to Equation (2.2) yields

$$i_{180°} = A(X_{180°} - \frac{B}{A} X'_{180°}) = 0 \quad ,$$

or

$$\frac{B}{A} = \frac{X_{180°}}{X'_{180°}} \quad . \tag{2.4}$$

Equation (2.4) now establishes the relationship required between the linear delay network elements if a unidirectional, polar response is to be obtained by the device.

Returning now to Figure 2.1, it can be seen that X_θ leads X'_θ by the phase angle φ. That is

$$X_\theta = X'_\theta \, e^{j\varphi} \quad .$$

Now,

$$\frac{\varphi}{2\pi} = \frac{Y}{\lambda} \quad ,$$

or

$$\varphi = \frac{2\pi y}{\lambda} = \frac{2\pi d \cos\theta}{\lambda} = (\frac{\omega d}{c})\cos\theta \quad , \tag{2.5}$$

since $y = d \cos\theta$.

Therefore,

$$X_\theta = X'_\theta e^{j\varphi} = X'_\theta e^{j(\omega d/c)\cos\theta} \quad . \tag{2.6}$$

Substituting Equation (2.6) into Equation (2.4) yields

$$\frac{B}{A} = \frac{X'_{180°}\, e^{-j(\omega d/c)}}{X'_{180°}} = e^{-j(\omega d/c)} \quad , \tag{2.7}$$

since $\cos 180° = -1$.

Now, inserting Equation (2.7) into Equation (2.2)

$$i_\theta = A[X_\theta - X'_\theta\, e^{-j(\omega d/c)}] \quad ,$$

and substituting the value of X_θ [Equation (2.6)] leaves

$$i_\theta = AX'_\theta[e^{j(\omega d/c)\cos\theta} - e^{-j(\omega d/c)}]$$

$$= AX'_\theta\{\cos[(\omega d/c)\cos\theta] + j\sin[(\omega d/c)\cos\theta] - \cos(\omega d/c) + j\sin(\omega d/c)\}$$

after expanding the exponentials into their respective cosine and sine terms.

If the value of the argument is required to be small, that is, if $\omega d/c \ll 1$, then the following simplifications can be made, namely,

$$\cos[(\omega d/c)\cos\theta] \to 1 \quad ,$$

$$\sin[(\omega d/c)\cos\theta] \to (\omega d/c)\cos\theta \quad ,$$

$$\cos(\omega d/c) \to 1 \quad ,$$

$$\sin(\omega d/c) \to (\omega d/c) \quad ,$$

and

$$i_\theta = AX'_\theta\,\{(1) + j[(\omega d/c)\cos\theta] - (1) + j(\omega d/c)\}$$

$$= AX'_\theta\, j[(\omega d/c)\cos\theta + (\omega d/c)]$$

or

$$i_\theta = jAX'_\theta\,(\omega d/c)\,(1 + \cos\theta) \quad . \tag{2.8}$$

The above expression holds reasonably well if $d < \lambda$ at the highest frequency of desired operation. That is,

$$\frac{\omega d}{c} = \frac{2\pi d}{\lambda} = \frac{2\pi\lambda/n}{\lambda} = \frac{2\pi}{n} < 1 \quad ,$$

where $n \approx 3$.

Now, if the absolute magnitudes of X_θ and X'_θ are not affected by diffraction, which means that the overall size of the device should be small when compared to a wavelength, then according to Equation (2.8) the device will produce a unidirectional, cardioid response.

Consider as the next step in the development of the theoretical model, a delay network, and not necessarily electrical, which must be capable of satisfying Equation (2.4). Figure 2.2a depicts a cross-sectional view of a hypothetical device, which, if examined closely, is identical to the mechanism described by Figure 2.1. The device is constructed of a two-part housing with a pressure gradient transducing element mounted on the center line. A cavity and a series of narrow slots are provided in the massive rear cover of the device. The slots are sealed off from the surrounding medium by a very thin neoprene acoustic window, which positively contains the "working fluid" (air, water, oil, etc.) in the rear cavity. The dimensions of the unit are chosen to give some predetermined front to back distance d, with d being $< \lambda$ to satisfy the condition of $\omega d/c \ll 1$. In addition, the acoustic pressures P_1, P_2, and P_3, which are approximately equal in magnitude but different in phase, act on the device as shown.

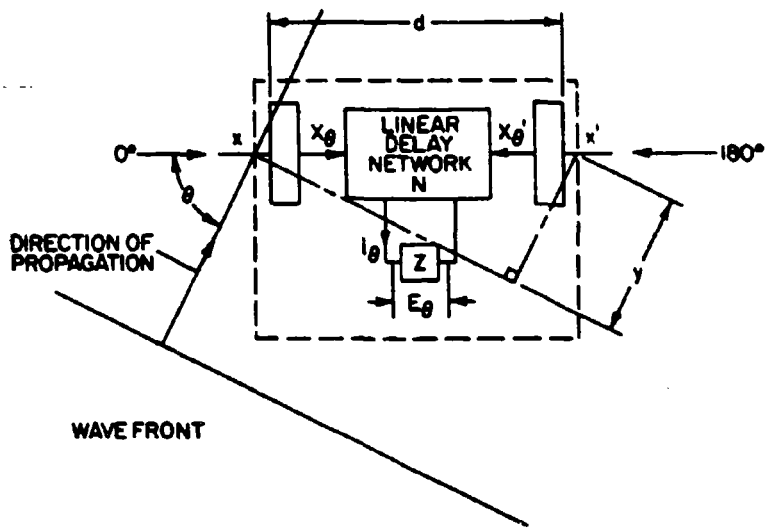

Figure 2.1. Diagram of the Theoretical Model

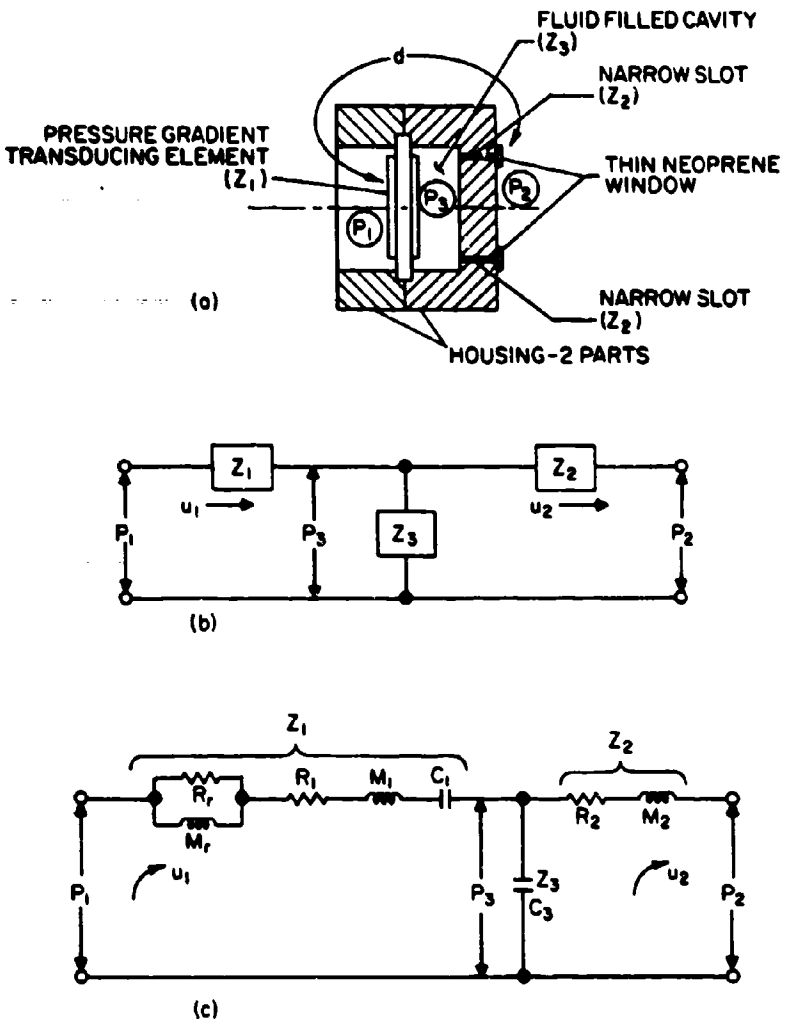

Figure 2.2. Analogous Acoustic Circuit of the Model

TABLE I

Analogous Circuit Relationships

Acoustical Quantity	Units	Electrical Quantity	Units
Acoustic Resistance - R_A	dyne-sec/cm^5	Resistance - R	ohm
Acoustic Inertance - M_A	gram/cm^4	Inductance - L	henry
Acoustic Compliance- C_A	cm^5/dyne	Capacitance - C	farad
Acoustic Impedance - Z_A=P/u	dyne-sec/cm^5	Impedance - Z=E/i	ohm
Acoustic Pressure - P	dyne/cm^2	Voltage - E	volt
Volume Velocity - u	cm^3/sec	Current - i	ampere
Volume Displacement - v	cm^3	Charge - Q	coulomb

Note: All circuit elements are constant and all variables are steady state RMS values.

Figure 2.2b is the effective analogous acoustic circuit for the device,[8,9] with Figure 2.2c defining the circuit in a little more detail, utilising the definitions of the acoustical components as defined in Table I. (Note: all impedances used in the text from this point on will be acoustical impedances. The acoustic subscript 'A' will be dropped from all symbols for simplicity.)

Referring to Figure 2.2b, the following network equations are obtained:

$$P_1 - u_1(Z_1 + Z_3) + u_2 Z_3 = 0 \qquad (2.9)$$

and

$$-u_2(Z_3 + Z_2) - P_2 + u_1 Z_3 = 0 \quad . \qquad (2.10)$$

Rearranging Equation (2.9)

$$-u_2 = -u_1 Z_1/Z_3 - u_1 + P_1/Z_3 \quad ,$$

and substituting into Equation (2.10)

$$-u_1 Z_1 + P_1 - u_1 \frac{Z_1 Z_2}{Z_3} - u_1 Z_2 + \frac{P_1 Z_2}{Z_3} - P_2 = 0$$

or

$$u_1[Z_1(1 + Z_2/Z_3) + Z_2] = (1 + Z_2/Z_3)\, P_1 - P_2 \quad .$$

Finally,

$$u_1 = \frac{(1 + Z_2/Z_3)\, P_1 - P_2}{Z_1(1 + Z_2/Z_3) + Z_2} \qquad (2.11)$$

After comparing Equation (2.11) with Equation (2.1), and remembering that the conventional electroacoustical analogy can be used, i.e., voltages and currents are analogous to acoustic pressures and volume velocities respectively (see Table I), it can be seen that A [the linear network coefficient of Equation (2.1)] is equivalent to the coefficient of P_1 divided by the denominator in Equation (2.11), and B (the second network coefficient) is equivalent to unity divided by the denominator. That is,

$$A = \frac{(1 + Z_2/Z_3)}{Z_1(1 + Z_2/Z_3) + Z_2} \quad , \tag{2.12}$$

and

$$B = \frac{1}{Z_1(1 + Z_2/Z_3) + Z_2} \quad . \tag{2.13}$$

Furthermore,

$$\frac{A}{B} = \frac{(1 + Z_2/Z_3)}{1} = 1 + \frac{(R_2 + j\omega M_2)}{(1/j\omega C_3)} = 1 + j\omega C_3 R_2 + j^2\omega^2 C_3 M_2 \quad , \tag{2.14}$$

and

$$\frac{A}{B} = (1 - \omega^2 C_3 M_2) + j(\omega C_3 R_2) \quad ,$$

where $Z_2 = R_2 + j\omega M_2$ and $Z_3 = 1/j\omega C_3$. If we set

$$M_2 = \frac{C_3 R_2^2}{2} \quad , \tag{2.15}$$

then

$$\frac{A}{B} = 1 - \left(\frac{\omega^2 C_3^2 R_2^2}{2}\right) + j(\omega C_3 R_2) \quad . \tag{2.16}$$

Realizing that the real terms on the right of Equation (2.16) are the first two terms of the Maclaurin series expansion of a cosine function, and that the imaginary term is the first term of the Maclaurin series expansion of a sine function, allows Equation (2.16) to be written

$$\frac{A}{B} = \cos \omega C_3 R_2 + j \sin \omega C_3 R_2$$

or

$$\frac{A}{B} = e^{j\omega C_3 R_2} \quad . \tag{2.17}$$

Therefore, equating Equation (2.7) and Equation (2.17) gives

$$\frac{A}{B} = e^{j(\omega d/c)} = e^{j\omega C_3 R_2}$$

or

$$\frac{d}{c} = C_3 R_2 \quad . \tag{2.18}$$

Equations (2.15) and (2.18) determine the interaction which must exist between the acoustic phase shift network, which is now seen to be composed of impedances Z_2 and Z_3, and between certain physical parameters of the device which are d, the front to back distance and c, the velocity of sound in the surrounding medium, if the device is to function as a unidirectional (cardioid) transducer.

CHAPTER III

INVESTIGATION

3.1 Acoustic Phase-Shift Network Requirements

The basic configuration and acoustic circuit of Figure 2.2 were initially employed to investigate the interrelationships which must exist between the acoustic phase-shift network elements and certain physical parameters of the device.

As has been shown, the phase-shift portion of the circuit consists of the acoustic impedances Z_2 and Z_3. The impedance Z_1 is attributed to the transducing element and to the transducer radiation impedance components, R_r and M_r. The volume of the rear cavity, coupled with the enclosed "working fluid" (which may be air, water, oil, etc.) combine to provide the value of Z_3.[10] That is,

$$Z_3 = \frac{1}{j\omega C_3} \tag{3.1}$$

where

$$C_3 = \frac{V}{\beta_f} \quad \text{(acoustic compliance - cm}^5\text{/dyne)} \quad . \tag{3.2}$$

The narrow slots in the rear enclosure provide the acoustic impedance Z_2. The acoustic impedance of a narrow slot[10] is given by

$$Z_2 = R_2 + j\omega M_2 \quad , \tag{3.3}$$

where

$$R_2 = \frac{12\mu_f \ell}{t^3 W} \quad , \tag{3.4}$$

$$M_2 = \frac{6\rho_f \ell}{5tW} \quad , \tag{3.5}$$

R_2 = acoustic resistance - dyne-sec/cm^5 ,

and

M_2 = acoustic inertance - gm/cm^4 .

However, limitations on the slot thickness[10] (which varies inversely as the square root of the frequency) are placed on the impedance expressions as defined by Equations (3.4) and (3.5). The values of the expressions hold reasonably well for slots that are kept relatively narrow. That is,

$$t < \frac{0.3}{\sqrt{\text{frequency}}} \tag{3.6}$$

3.1.1 Working Fluid. The device under investigation in this study was to be designed for an underwater application. Attempts to satisfy the basic relationships [Equations (2.15), (2.18), and (3.2)] for an underwater device presented problems which do not normally exist in an air environment. For example, selecting air as the network working fluid (as is done in microphone work) required the volume of the rear cavity and, therefore, d to be impractically large in order to satisfy the

phase-shift network parameters. The compliance of an air-filled cavity would also deviate drastically with changes in the hydrostatic pressure. Hence, the acoustic impedance Z_3 created by the cavity and the air would be depth sensitive. Past experiences have also proven that air pressure compensating systems, which theoretically could be used to maintain a constant pressure, turn out to be bulky and, for the most part, unreliable. In addition, all of the acoustic circuit relationships could not be satisfied due to the inherent low value of μ_f, the dynamic viscosity of air.

When consideration was given to using water as the working fluid (to free-flood the rear cavity) only the problem of the depth-sensitive compliance was eliminated. The acoustic network incompatibilities still remained. In other words, water would not provide the proper phase shift. A complete literature search was then initiated to try to uncover a material, preferably a liquid, which would possess the physical characteristics that would satisfy the three basic phase-shift network equations,

$$R_2 = \frac{d}{cC_3} \quad , \tag{2.18}$$

$$M_2 = \frac{C_2 R_2^2}{2} \quad , \tag{2.15}$$

$$C_3 = \frac{V}{\beta_f} \quad , \tag{3.2}$$

and which would also provide a reasonably small overall size of the device.

A Dow-Corning 200 (200 centistoke) silicone oil with the physical characteristics listed in Table II was found to completely satisfy the acoustic phase-shift network requirements. The requirements were determined in the following manner:

The numerical values of R_2 and M_2 were obtained by evaluating Equations (3.4) and (3.5), which are

$$R_2 = \frac{12\mu_f \ell}{t^3 W} \tag{3.4}$$

and

$$M_2 = \frac{6\rho_f \ell}{5tW} \quad . \tag{3.5}$$

The slot width (W) and the slot length (ℓ) were both fixed by the geometry of the device. The dynamic viscosity (μ_f) and the density (ρ_f) of the silicone oil were also fixed, for constant temperature and pressure conditions, which then left the slot thickness t as the only independent variable.

Numerical values for R_2 and M_2 had to be chosen for the network in such a manner that the basic phase-shift network equations

$$M_2 = \frac{C_3 R_2^2}{2} \tag{2.15}$$

and

$$\frac{d}{c} = C_3 R_2 \tag{2.18}$$

would be satisfied. The choice was made in the following manner: the acoustic compliance (C_3) was first eliminated in Equations (2.15) and (2.18), giving

TABLE II

Properties of Dow-Corning 200 Silicone Oil

Temperature (^{o}C)	Pressure (psia)	Density ρ_f (gm/cm^3)	Velocity of Sound c_f (cm/sec)	Kinematic Viscosity ν_f (cm^2/sec)	Dynamic Viscosity μ_f (gm/cm-sec)	Adiabatic Bulk Modulus β_f ($dyne/cm^2$)	Coefficient of Expansion α ($cm/cm/^{o}C$)
25	14.7	.970	1.00×10^5	2.00	1.94	$.970 \times 10^{10}$	.00096
20	14.7	.980	1.015×10^5	2.30	2.26	1.01×10^{10}	.00096
15	14.7	.995	1.031×10^5	2.55	2.54	1.06×10^{10}	.00096
10	14.7	1.015	1.047×10^5	2.90	2.94	1.112×10^{10}	.00096
5	14.7	1.050	1.063×10^5	3.15	3.30	1.185×10^{10}	.00096

$$M_2 = \frac{d\,R_2}{2c} \quad . \tag{3.7}$$

The acoustic resistance (R_2) and the acoustic inertance (M_2), which are given by Equations (3.4) and (3.5), were then substituted into Equation (3.7) and the resulting equation was solved for the slot thickness t. That is,

$$\frac{6\rho_f \ell}{5tW} = \frac{12d\mu_f \ell}{2c\,t^3 W}$$

and

$$t = \sqrt{\frac{5\mu_f d}{\rho_f c}} \quad , \tag{3.8}$$

where c, the velocity of sound in the surrounding medium (in this case water) was fixed and where the front-to-back distance d was chosen to be 10 cm, small enough to satisfy the limit $d < \lambda$. The slot thickness t calculated from Equation (3.8) will now give values of R_2 and M_2 that will satisfy the basic phase-shift network equations.

Next, the volume of fluid (V) required to give the specified compliance (C_3) and, hence, the required size of the rear cavity was determined. The acoustic compliance (C_3) was again eliminated between Equations (3.2) and (2.18), resulting in Equation (3.9),

$$V = \frac{d\beta_f}{cR_2} \quad . \tag{3.9}$$

Equation (3.9) then fixed the relative size of the rear cavity of

the device, in addition to providing the specified phase-shift network compliance. Again, the velocity of sound c and the front-to-back distance d were both fixed.

All basic phase-shift network requirements are now satisfied. In addition, it is recalled that the overall physical size of the device must also be kept small, when compared to a wavelength, in order to overcome diffraction effects. Therefore, the network components are specified as follows:

For a Dow-Corning 200 (200 cs) silicone oil at 15°C and at atmospheric pressure, and with d, the front-to-back distance chosen as 10 cm,

$$t = 0.028 \text{ cm} \qquad \text{[From Equation (3.8)]}$$

with

$$\ell = 1 \text{ cm},$$

$$W = 26.7 \text{ cm},$$

$$R_2 = 45{,}000 \ \ (\text{gm/cm}^4\text{-sec}) \qquad \text{[From Equation (3.4)]},$$

$$M_2 = 1.55 \ \ (\text{gm/cm}^4) \qquad \text{[From Equation (3.5)]},$$

and

$$V = 16.3 \text{ cm}^3 \qquad \text{[From Equation (3.9)]}.$$

3.1.2 Temperature and Pressure Considerations. The density (ρ_f), the dynamic viscosity (μ_f), and the adiabatic bulk modulus (β_f) are three terms in the network equations which depend upon the ambient temperature and pressure and can therefore be expected to affect the performance of the phase-shift network. An attempt was made to assess the effect on the overall performance of the

phase-shift network due to variations of the above parameters with temperature and pressure.

Figure 3.1 shows the variation of the acoustic resistance (R_2) and the acoustic inertance (M_2) of a thin slot, filled with the Dow-Corning 200 (200 cs) silicone oil, with the slot thickness t as the variable. The solid and the dashed curves present the values of R_2 and M_2 at temperatures of 25°C and 5°C (the approximate extremes of temperature in the ocean). As can be seen, over this temperature range, the percentage changes of the values of R_2 and M_2 are approximately 8 percent and 4 percent, respectively.

The variation of the acoustic compliance (C_3) with temperature, which is given by Equation (3.2), depends primarily on the variation of the adiabatic bulk modulus (β_f), the change in the original volume (V_o) being so small that it may be neglected. Best estimates, using data obtained from the available literature, indicate that the compliance (C_3) will vary approximately 22 percent over this same (25°C to 5°C) temperature range. In spite of the variations in R_2, M_2, and C_3, the experimental results presented in Section 4.2.4 indicate that, for a temperature change of 22°C to 14°C, there was no measurable change in the directivity patterns of the transducer model.

Variations of the acoustic resistance (R_2) and the acoustic inertance (M_2) due to a pressure change of 0 to 1000 psig (0 to 2300 ft of water) are significantly smaller in magnitude than the corresponding changes due to the above temperature change of 25°C

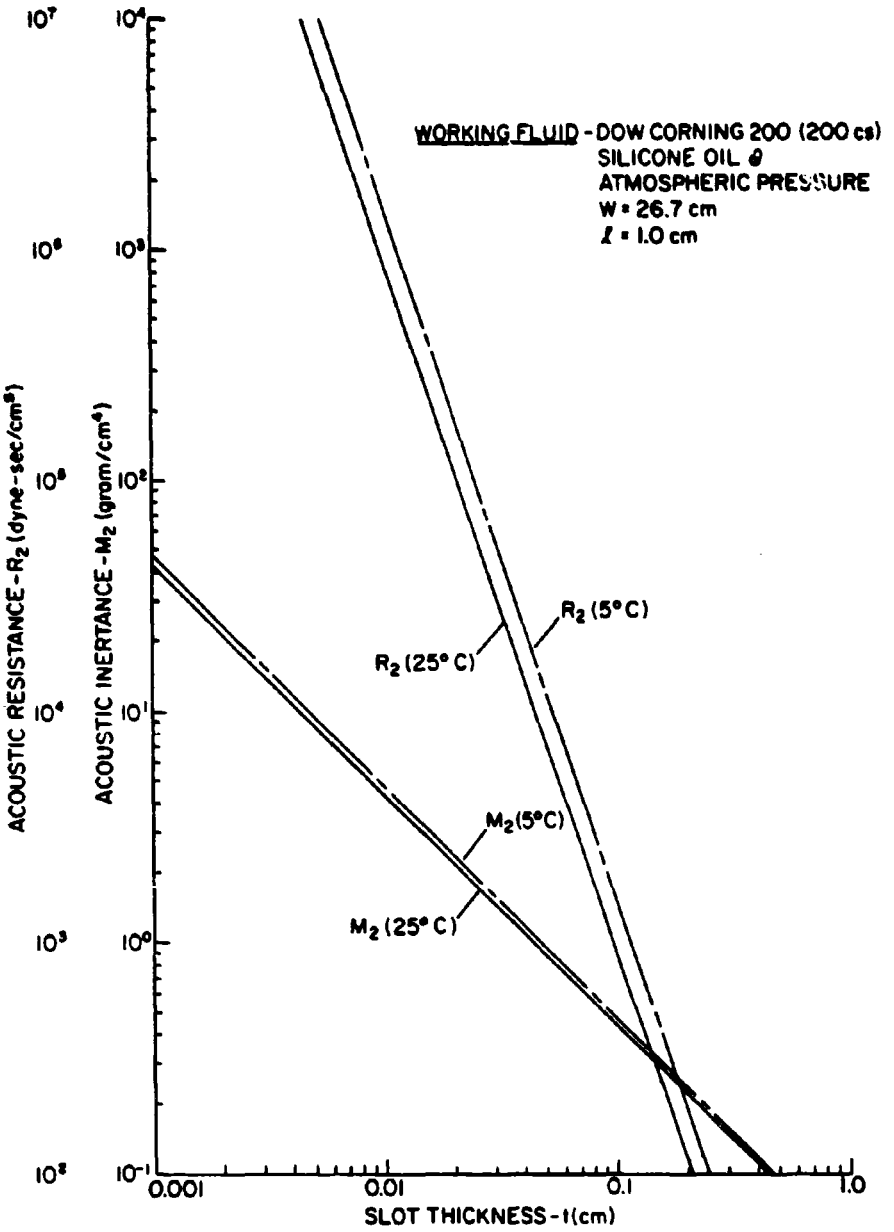

Figure 3.1. The Acoustic Resistance and Acoustic Inertance as a Function of Slot Thickness

to 5°C. The inertance (M_2) due to the change in density (ρ_f) will vary less than 1 percent. There appears to be no available data on the effect of pressure on the dynamic viscosity (μ_f) of the silicone oil. However, Dodge and Thomson[14] state that the dynamic viscosity (μ_f) of many lubricating oils remains relatively stable for pressure changes of this magnitude.

The variation of the acoustic compliance (C_3) with pressure, which depends primarily upon a change in the adiabatic bulk modulus (β_f), will vary approximately 9 percent over this pressure range. Since these percentage changes due to pressure variations are less than or comparable to the corresponding changes due to the temperature variation of 14°C to 22°C, it appears reasonable to predict that no appreciable change in performance should occur over this pressure range.

3.2 Transducer Model Design

Figure 3.2 shows the unidirectional transducer model which was constructed to test the validity of the theoretical model. The overall dimensions of the model (8.55 cm O.D. x 3.64 cm long) were kept to a minimum to keep the device small when compared to a wavelength. The transducer, as shown, was constructed of a two-part, cold-rolled steel housing (A and B) and a massive, lead-loaded, movable rear cone (C).

Johnson and Woollett,[12] in their paper on flexural ceramic disk transducers, stress that the transducer housing should be made stiff enough so that the enclosed volume does not change appreciably

as the disk vibrates. They recommend that the housing should be designed so that the volume velocity of the housing would be less than approximately 15 percent of the volume velocity of the radiating front face of the disk. This should prevent the back of the disk from radiating appreciably.

It was impossible to rigidly fasten the rear cone (C) in this particular design, since the investigation required that the slot thickness (t) be adjustable in order to experimentally determine the required slot thickness. Therefore, the rear cone was allowed to "float" against the resisting spring (I) which effectively placed a mass reactance term in shunt with the compliance C_3 of Figure 2.2c. At frequencies below those for which these two reactances are equal in magnitude, the mass reactance acts as the principal controlling element in the circuit and at frequencies above those for which these two reactances are equal in magnitude, the compliance C_3 acts as the principal controlling element. Therefore, the mass of the rear cone, for this design, should be made as large as practical so that it does not effectively shunt C_3. This mass was made large enough for the desired frequency range (4000 Hz to 6000 Hz) simply by adding additional mass, in the form of a lead slug, to the rear cone. Thus, the acoustic impedance due to the rear cone mass was sufficiently greater than the acoustic impedance due to the fluid compliance. That is,

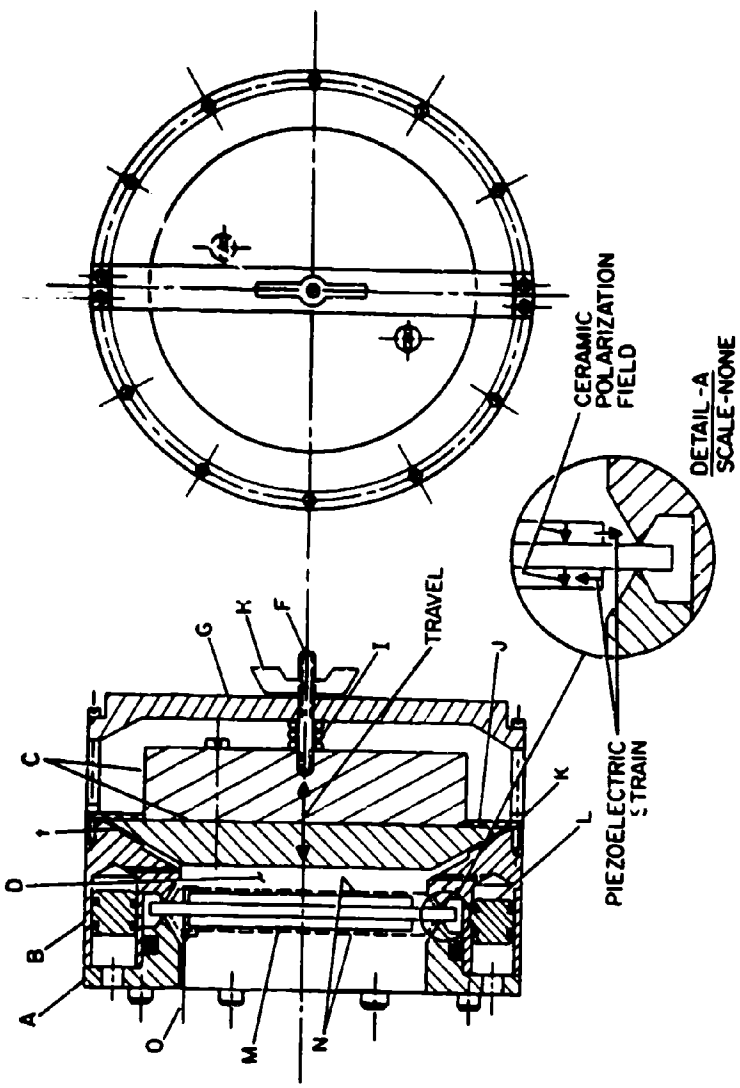

Figure 3.2. Cross-Sectional View of the Transducer Model

$$j\omega M_{A\text{-CONE}} > \frac{1}{j\omega C_{A\text{-CAVITY}}}$$

between 4000 Hz and 6000 Hz.

Now,

$$M_{A\text{-CONE}} = \frac{m_{CONE}}{S^2} = 2.63 \text{ grams/cm}^4 \quad ,$$

where m_{CONE} = 1375 gms = total mass (including lead slug) of the cone, $S = 22.85 \text{ cm}^2$ = cross-sectional area of the rear cavity, and

$C_{A\text{-CAVITY}} = C_3 = 1.51 \times 10^{-9}$. [From Equation (3.2)]

Therefore, at 4000 Hz,

$$\omega M_{A\text{-CONE}} = 6.6 \times 10^4$$

and

$$\frac{1}{\omega C_{A\text{-CAVITY}}} = 2.65 \times 10^4 \quad .$$

At 6000 Hz,

$$\omega M_{A\text{-CONE}} = 9.0 \times 10^4$$

and

$$\frac{1}{\omega C_{A\text{-CAVITY}}} = 1.76 \times 10^4 \quad .$$

Thus, the mass reactance of the cone is 2½ to 4 times greater than the stiffness reactance of the cavity for this frequency range of 4000 Hz to 6000 Hz.

Having established the design parameters with this experimental model, a practical design could be made to have a rigid rear cone mass and appropriate slot dimensions, thus eliminating the shunting effect of the floating rear cone mass.

The acoustic phase-shift network elements [the silicone oil-filled rear cavity (D) and the dimensions of the peripheral narrow slot (t)] were chosen to satisfy the requirements of Section 3.1.1. The movable rear cone, as previously mentioned, was provided to allow adjustment of the slot thickness (t). This, of course, allowed the value of the impedance $Z_2 = (R_2 + j\omega M_2)$ to be adjusted slightly in the following manner. The rear cone was aligned in the mating cavity of the housing (B) by a closely machined shaft (F) which was securely mounted to the rear cone (C) and which passed through a closely machined clearance hole in the framework (G). The shaft (F) also had a 5-40 unc-2 thread turned into one end portion. Linear travel of the rear cone (see arrow) was provided by turning the wing nut (H), which pulled the cone against the compression spring (I), and for every complete turn of the wing nut, the cone traveled 0.0762 cm. Adjustment of the impedance Z_2 was accomplished by the movement of the cone which changed the slot thickness (t).

The volume of the rear cavity (16.5 cm^3), as required in Section 3.1.1, was filled with a "working fluid" of Dow-Corning '200' Silicone Oil with a 200-centistoke dynamic viscosity rating. A thin (0.038 cm thick) acoustic window (J), molded from a pc neoprene rubber, was cemented to the rear cone and then fastened to the housing (B) via the clamp ring (K). The main function of the window was to contain the silicone oil and to allow the sound wave to pass unimpeded into the phase-shift network slot (t). It also served

another purpose in that it prevented the rear cone from rotating about the central axis of the transducer.

The housing (B) also contained two free-floating piston accumulators (L) with ample reservoir volume (0.778 cm^3) which were open to the ambient sea pressure on one side and which were suitably interconnected by very small, high impedance (0.038 cm diameter) holes to the oil-filled rear cavity (D). The accumulator system was used to equalize the pressure inside the cavity (D) to the ambient hydrostatic pressure. In this manner, the transducer was rendered depth insensitive, since there would be no pressure differential across the transducing element (M) causing it to fracture. In addition, the accumulators also compensated for changes in fluid volume which would occur due to a change in the ambient temperature. The small diameter, high impedance interconnecting holes were required so that there would be only one unimpeded sound path into the rear cavity (D), that is, via the phase-shift network narrow slot (t). A check of the impedance provided by the hole showed that it was approximately 1000 times greater than the impedance (Z_2) of the phase-shift slot.

Since the transducer was to be primarily designed for a low frequency application (3000 Hz to 6000 Hz in water), a trilaminar, flexural piezoceramic disk was selected for the pressure gradient transducing element (M). The flexural disk (M)[11,12] was constructed as a three-layer sandwich, with the two outer layers of a PZT-4 type piezoelectric ceramic. The inner section of the element was

made of a 6061-T6 aluminum disk and its outside diameter was larger than the ceramic outside diameter to provide a suitable edge mounting as shown in Detail A of Figure 3.2. The two ceramic disks were oriented and cemented to the inner aluminum disk in such a manner that their polarization fields were in the same direction (Figure 3.2, Detail A). The ceramics were then parallel-connected; the electrodes connected to the aluminum disk forming one terminal and the outer electrodes joined together to form the other terminal. Thus, a voltage applied across these terminals would produce strains of opposite sense in the piezoceramic disks, causing the trilaminar disk to flex and function as a sound projector, or to produce an electrical output when driven flexurally by an impinging sound wave to serve as a hydrophone.

Particular attention was paid to the exact mounting of the trilaminar disk. (See Figure 3.2, Detail A.) The disk was centered and then pinched between the two Vee-shaped circular wedges which were machined in part A and part B of the housing. Part A was then rigidly fastened to housing part B by eight socket-head cap screws. This type of mounting provided a simply supported boundary condition which, according to theory,[12] would provide an optimum effective electromechanical coupling coefficient for the transducer. It also permitted the element to be modeled theoretically as a thin plate with a simply supported boundary. In addition, it was determined experimentally (on various trilaminar arrangements) that this type of mounting also isolated the trilaminar disk from the housing

extremely well, which left the device relatively free from pick-up due to mechanical excitation of the housing.

The trilaminar disk was given a thin (0.038-0.051 cm) polyurethane coating (N) on both sides to electrically insulate the piezoceramic disks after the proper lead (0) connections had been made. A photograph of the completely assembled model is shown in Figure 3.3.

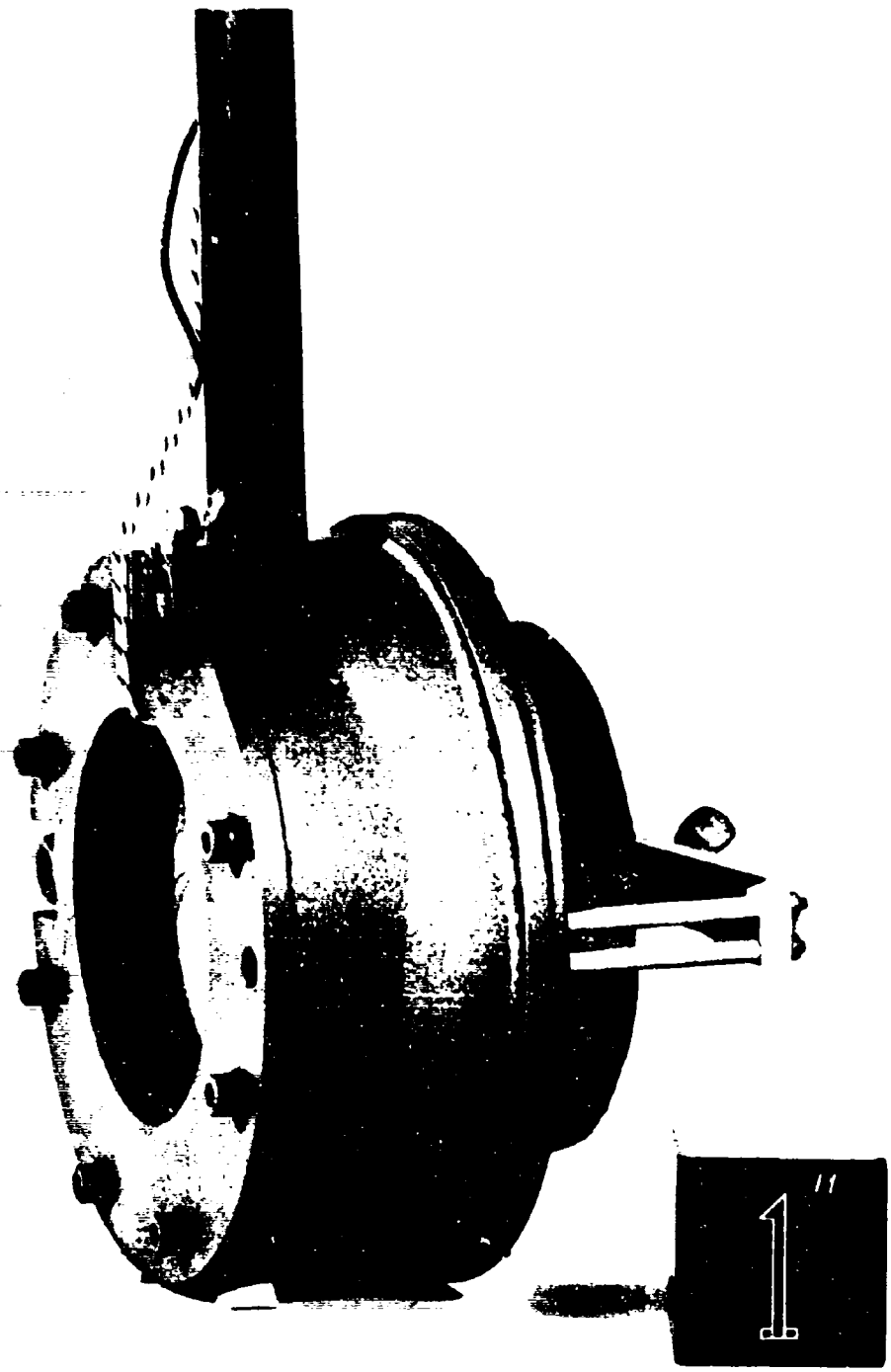

Figure 3.3. The Transducer Model

CHAPTER IV

EXPERIMENTAL PROCEDURE AND RESULTS

4.1 Experimental Procedure

The following steps were undertaken to evaluate the transducer model. Experimental data, in the form of azimuth directivity patterns (polar responses) were obtained with the transducer model in four design configurations or stages. That is, directivity patterns of the model were taken:

a. Without the acoustic phase-shift network. (The model was simply a dipole receiver.)

b. With the acoustic phase-shift network; the working fluid used in the rear cavity being air.

c. With the acoustic phase-shift network; the working fluid used in the rear cavity being fresh water.

d. With the specified acoustic phase-shift network; the working fluid used in the rear cavity being the Dow-Corning 200, 200 centistoke, silicone oil.

The major portion of the experimental work was conducted using the Ordnance Research Laboratory's water-filled anechoic tank facility.[13] This concrete tank (which is 20 ft long, 12 ft wide, and 15 ft deep) is lined with insulkrete wedges to reduce reflections at the boundaries. The average water temperature of

the tank was approximately 22°C. The projector-hydrophone depth was set at 60 inches, while the projector-hydrophone separation was 48 inches for most of the experimental measurements. Other separations were also used.

A Scientific-Atlanta Automatic Transmission Measuring System, as shown by the block diagram of Figure 4.1, was used to record the experimental data.

As indicated by Figure 4.1, the output of an oscillator was fed to a Transmit Signal Gate which was controlled by a Pulse Timing Generator. The Pulse Timing Generator's function was to set the pulse widths and pulse repetition rates that were to be used.

The output of the controlled Transmit Signal Gate was then transferred to a Preamplifier which in turn fed a main Power Amplifier. The output of the Power Amplifier, which was kept at a constant level by a Voltage Current Normalizer, was then fed to the projector. A Naval Research Laboratory-Underwater Sound Reference Division, F-33 Transducer was used as the projector for the experiment.

The received signal output of the hydrophone, which was the transducer model in this case, was first preamplified and then fed through a Line Driver which served as an impedance-matching network. The Line Driver matched the output impedance of the hydrophone to the input impedance of the Scientific-Atlanta System. The signal out of the Line Driver Network was filtered (a band pass of 2000 Hz to 10,000 Hz was used), fed to a Receiver Signal Gate, and then to a

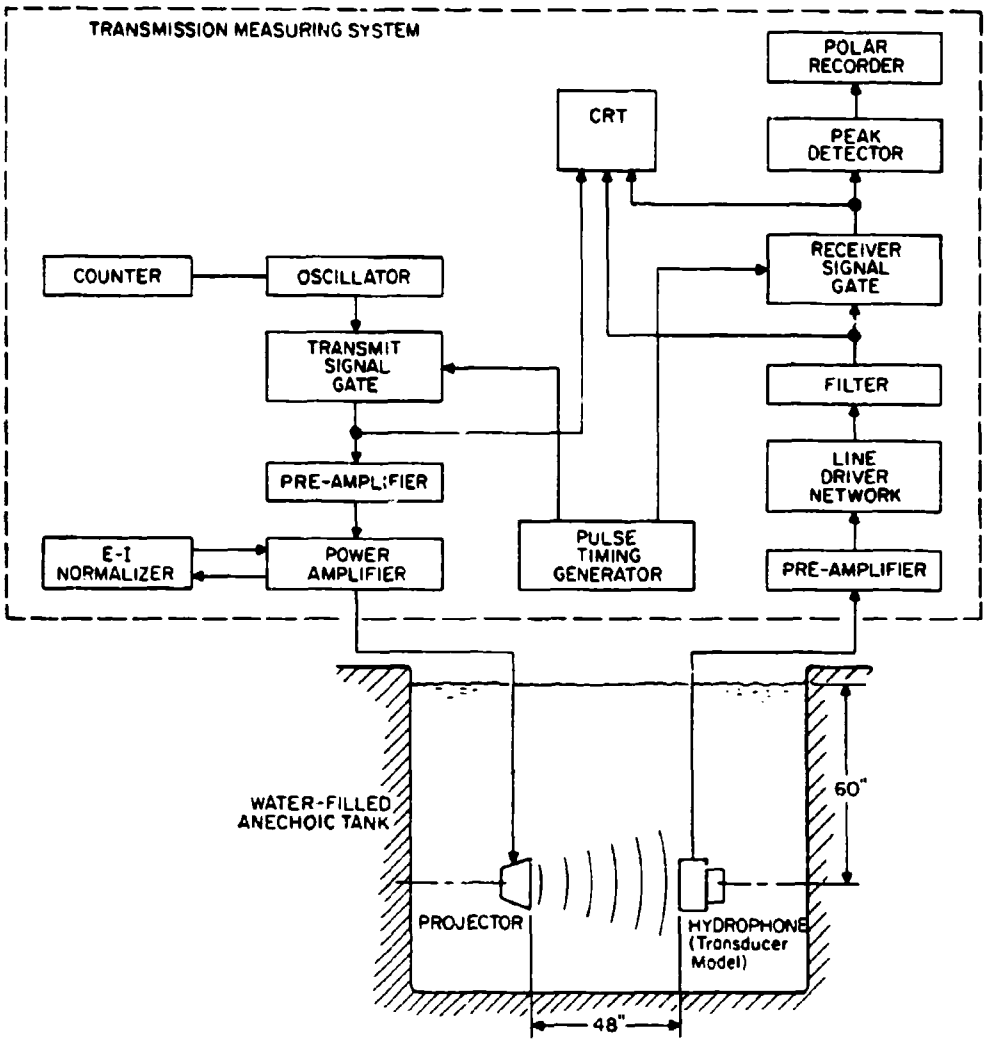

Figure 4.1. Block Diagram of the Experimental Set-up

Peak Detector Network. The timing of the Receiver Signal Gate was, like the Transmit Signal Gate, controlled by the Pulse Timing Generator. Finally, the output of the Peak Detector was fed to a Polar Recorder and the output was plotted. A constant visual check on all of the gating and timing functions as well as on the received signal wave form, was maintained by utilizing a Cathode Ray Oscilloscope as shown.

Due to the physical size limitation of the anechoic tank, pulsed calibration techniques were required so that the measured directivity pattern of the model would be independent of reflection and standing wave phenomena. The data (directional polar patterns) were verified experimentally to be independent of the relative positions of the projector and the model in the tank simply by setting the projector and the model at various center-to-center separations and then re-recording. Likewise, responses were also recorded with the projector and model at different depth level settings in the tank. The resulting repeatability of the data (for center-to-center separations of 48, 60, 72, and 84 inches and for depth level settings of 48, 60, and 84 inches) was within ±1 dB.

A final calibration of the model, which included a free-field voltage response (M_o) in addition to the directivity patterns, was made at the Ordnance Research Laboratory's Black Moshannon Calibration Station. The experimental set-up was identical to the anechoic tank set-up except that a CW sound field was used. The body of water available at the Calibration Station was large enough

to avoid reflection and standing wave phenomena with a CW sound field. The average water temperature was approximately 14°C for these measurements and the projector-hydrophone depth was set at 84 inches. Various projector-hydrophone separations (60 inches to 120 inches) were also tried with insignificant variation of the data.

4.2 Results

4.2.1 Transducer Model Without Phase-Shift Network. Figure 4.2 shows the measured directivity pattern of the transducer model at 5100 Hz without the acoustic phase-shift network. The result was a bidirectional or cosine pattern, as expected, since the transducer acts as a simple dipole in this configuration.

Figures 4.3 and 4.4 were recorded at 4000 Hz and 6000 Hz, respectively, with all conditions such as projector voltage, amplifier levels, projector and model separation, etc., being identical to the conditions under which Figure 4.2 was recorded. The plots are practically identical, indicating only minor changes with frequency.

4.2.2 Transducer Model with Phase-Shift Network; Working Fluid - Air. The directivity pattern shown by Figure 4.5 recorded the response of the model at 5159 Hz with the acoustic phase-shift network in place but with air used as the working fluid in the rear cavity. The phase-shift slot thickness t in this case was set equal to zero; that is, the slot was closed. The response was

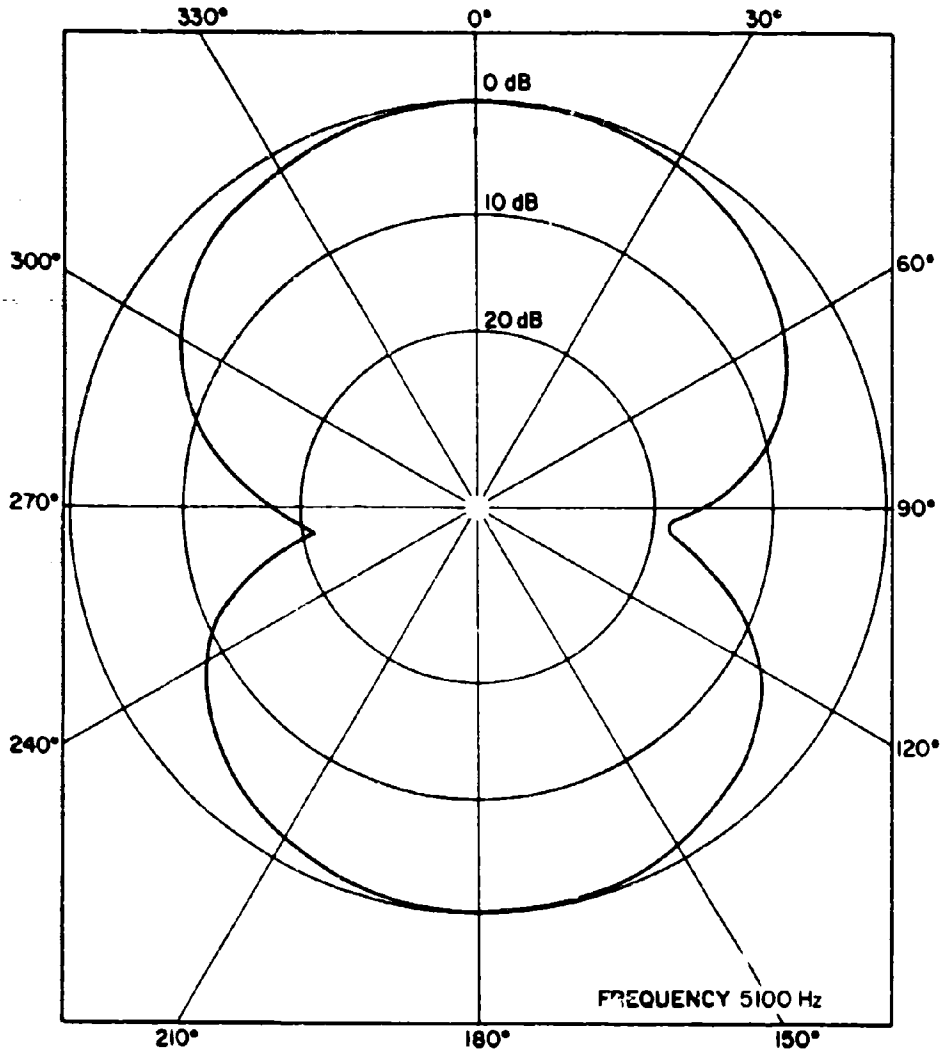

Figure 4.2 Directivity Pattern at 5100 Hz Without the Acoustic Phase-Shift Network

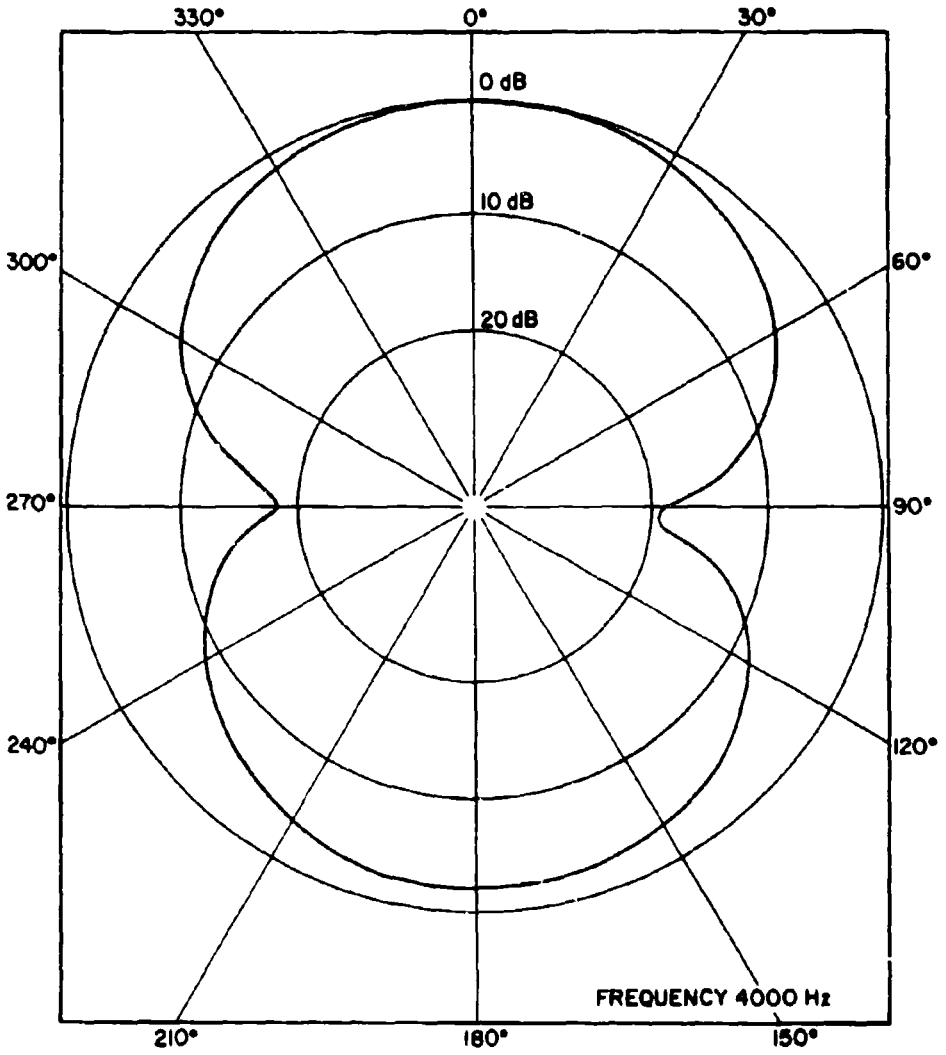

Figure 4.3. Directivity Pattern at 4000 Hz Without the Acoustic Phase-Shift Network

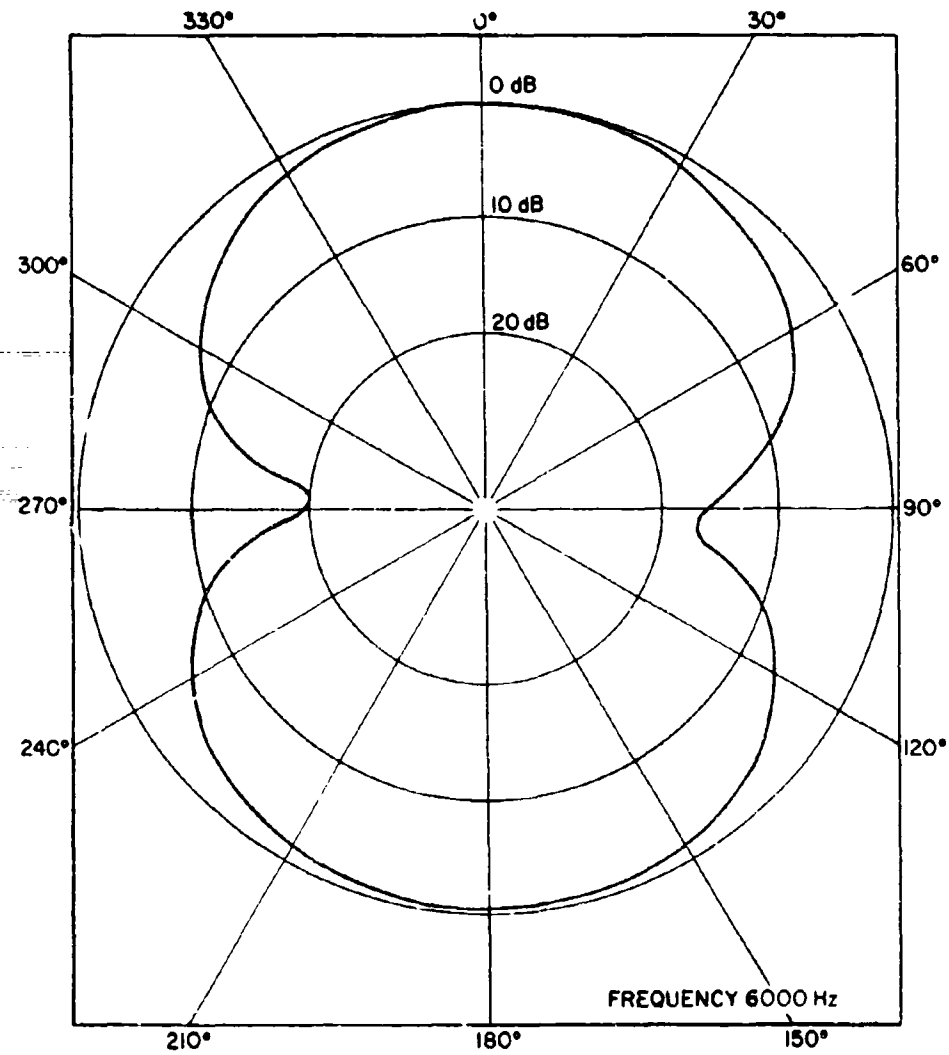

Figure 4.4. Directivity Pattern at 6000 Hz Without the Accustic Phase-Shif' 'etwork

omnidirectional for this condition since the transducer behaves as a simple source (its dimensions being small when compared to the wavelength) radiating only in the forward direction.

Directivity responses were taken at other frequencies and with the slot thickness set at a variety of other dimensions (0.0025 to 0.254 cm) with no indication of a unidirectional cardioid response present. The resulting plots, as expected, were all omnidirectional since the transducer behaves as a simple source for all slot thickness dimensions chosen when air was used as the working fluid in the rear cavity. That is, the radiation from the rear of the transducer housing was not well coupled to the medium due to the highly compliant air backing of the rear cavity.

4.2.3 Transducer Model with Phase-Shift Network; Working Fluid - Water. Note: The thin acoustic window (J of Figure 3.2) was removed for this series of responses, to allow the rear cavity to free-flood with water.

The response of the transducer model at 5056 Hz with the slot thickness set at 0.[illegible] m (relatively wide open) is shown in Figure 4.6. The resulting pattern was bidirectional. Figure 4.7 shows a response with the slot closed. As can be seen, the pattern is not completely omnidirectional as it should be. This lack of omnidirectional response is attributed to the extremely high stiffness of the water-filled rear cavity which actually couples and drives the rear cone mass. Apparently the slot is really never closed and rear radiation, as shown by the partial bidirectional pattern, results.

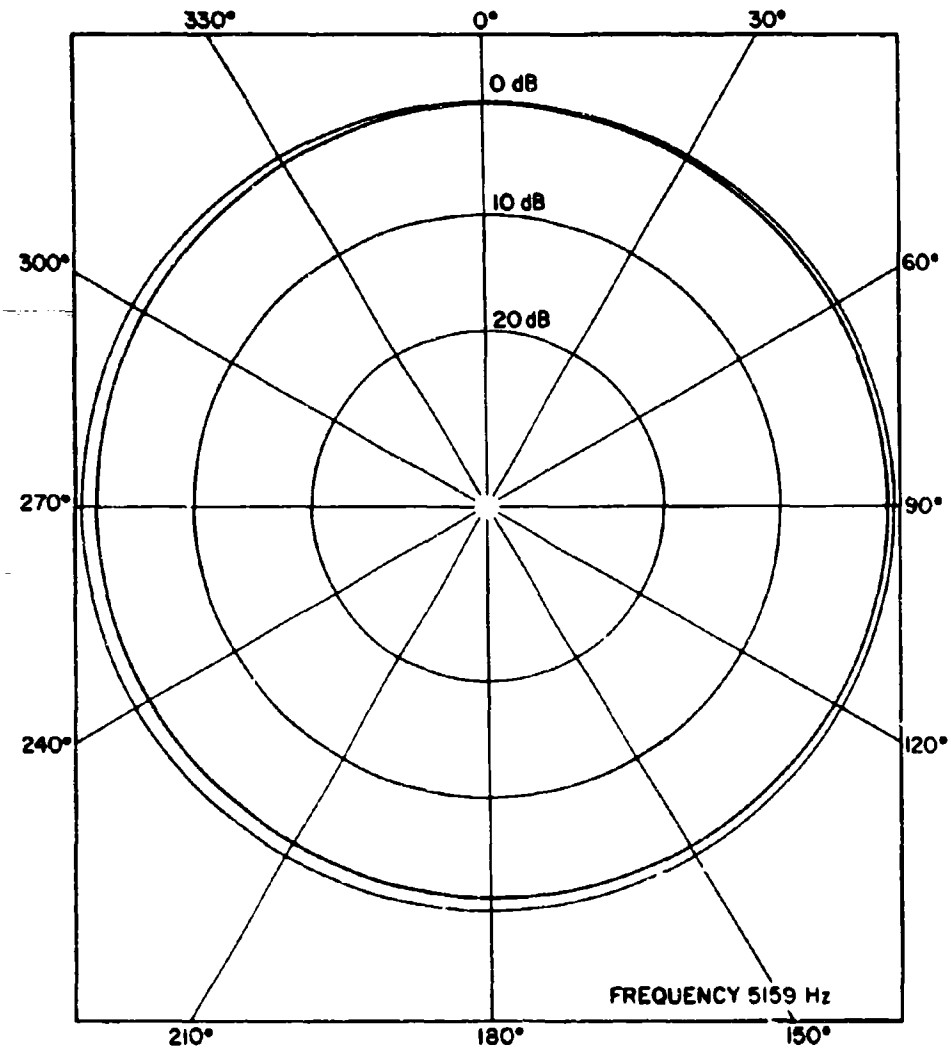

Figure 4.5. Directivity Pattern at 5159 Hz With an Air-Filled Acoustic Phase-Shift Network (t = 0 cm)

Directivity responses made at various frequencies and with a variety of other slot dimensions (0.0025 to 0.254 cm) were also recorded with no unidirectional results being obtained. The resulting plots were bidirectional, but moderately approaching omnidirectionality as the slot thickness was reduced to zero.

4.2.4 Transducer Model with Specified Phase-Shift Network Parameters. The directivity pattern shown by Figure 4.8 was recorded at 5014 Hz with the acoustic phase-shift network as specified in Chapter III. The rear volume was filled with the Dow-Corning 200 (200 cs) silicone oil working fluid. The slot thickness, t, was set at the computed value of 0.028 cm. A unidirectional, cardioid response with a front-to-back discrimination of 18 dB resulted. Figures 4.9, 4.10, and 4.11 were recorded at 5320 Hz, 5507 Hz, and 6023 Hz, respectively. The required unidirectional response with front-to-back discriminations of 27 dB, 22 dB, and 17 dB were obtained as shown. Figures 4.12, 4.13, and 4.14 were recorded at 4910 Hz, 4510 Hz, and 4008 Hz, and they also show a unidirectional response with front-to-back discriminations of 18 dB, 16 dB, and 10 dB.

Figures 4.15 and 4.16 are directivity patterns of the model with the slot thickness, t, set at 0 and at 0.254 cm. As expected, omnidirectional and bidirectional responses, respectively, were obtained with the phase-shift slot set at these two extremes. Therefore, the model functioned as predicted only when the specified, phase-shift network parameters were used.

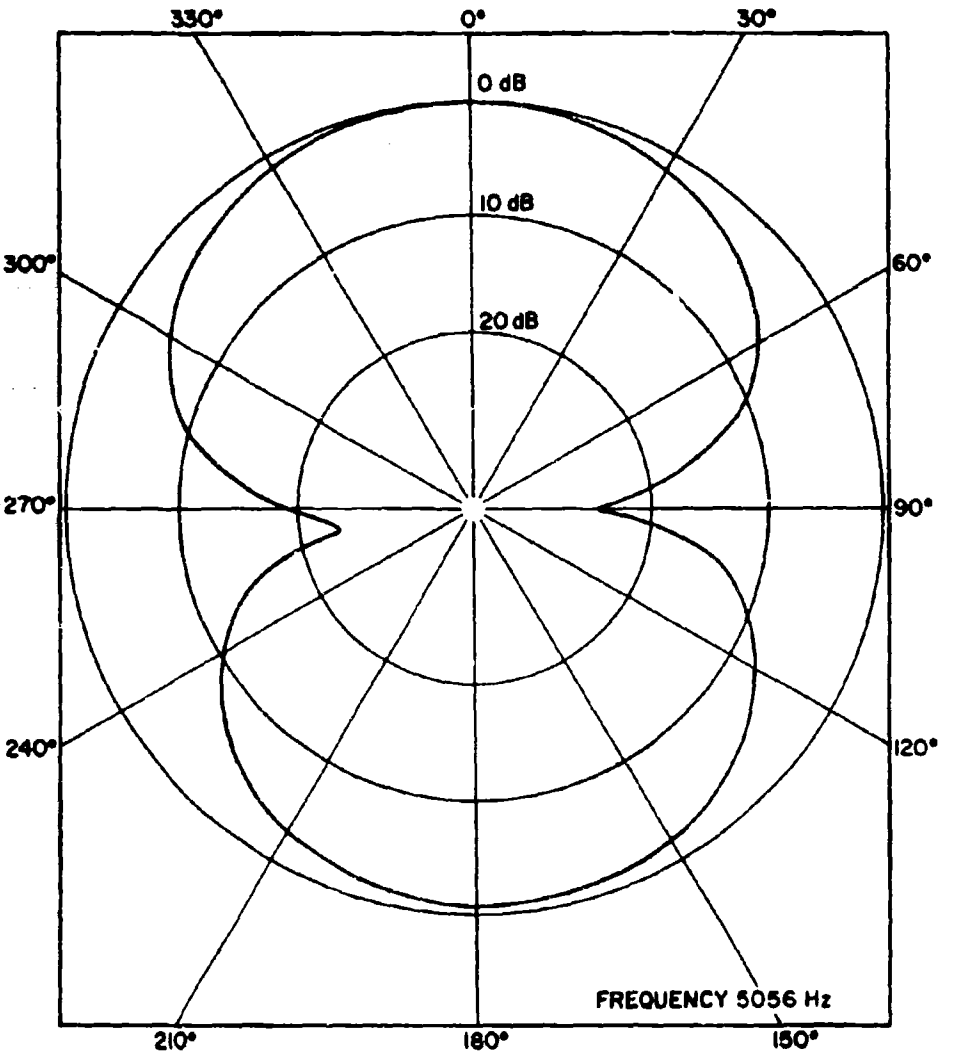

Figure 4.6. Directivity Pattern at 5056 Hz With a Water-Filled Acoustic Phase-Shift Network (t = 0.216 cm)

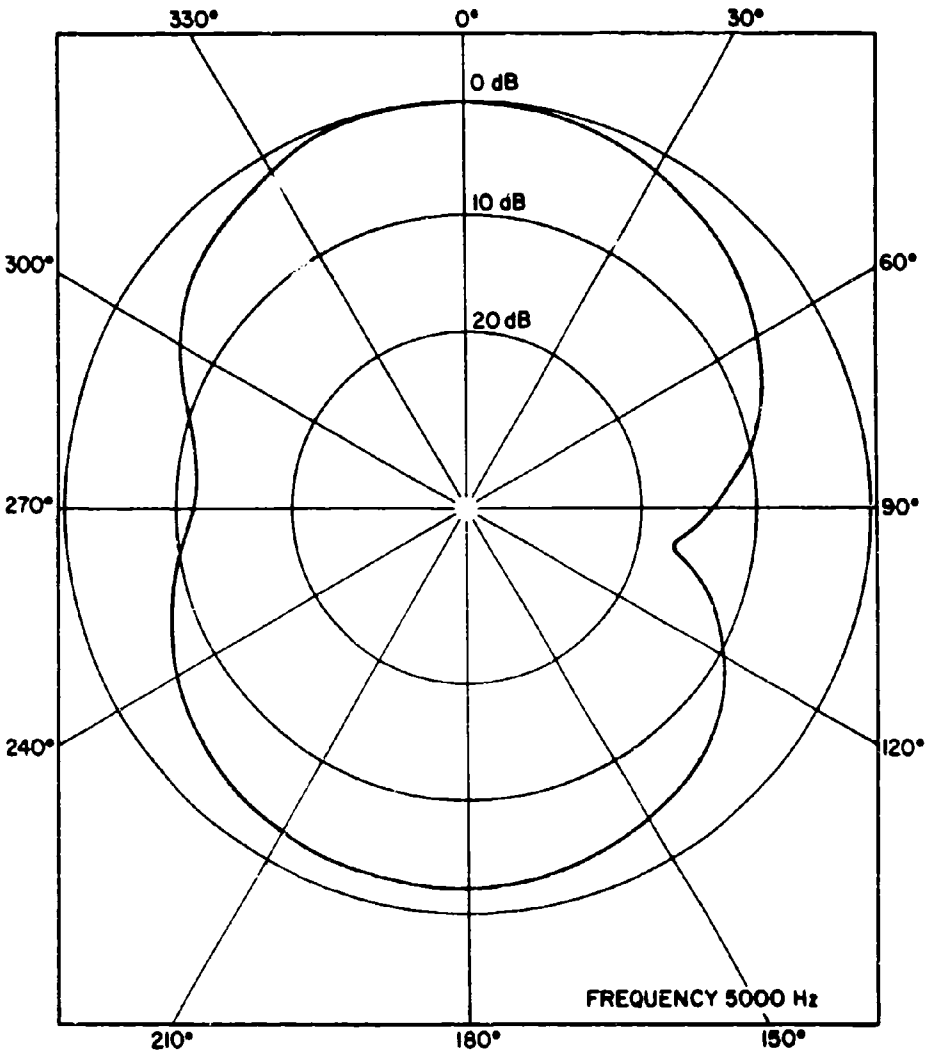

Figure 4.7. Directivity Pattern at 5000 Hz With a Water-Filled Acoustic Phase-Shift Network (t = 0 cm)

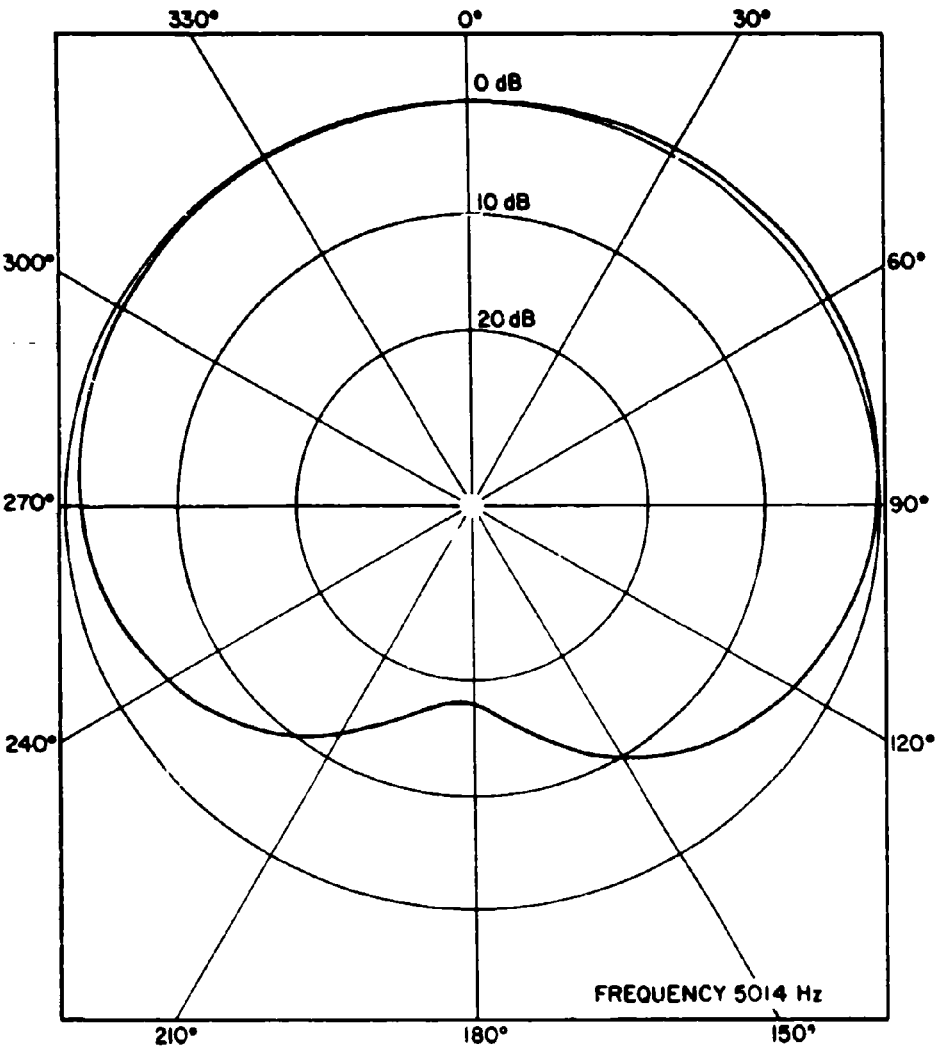

Figure 4.8. Directivity Pattern at 5014 Hz With the Specified Acoustic Phase-Shift Network Parameters (t = 0.028 cm)

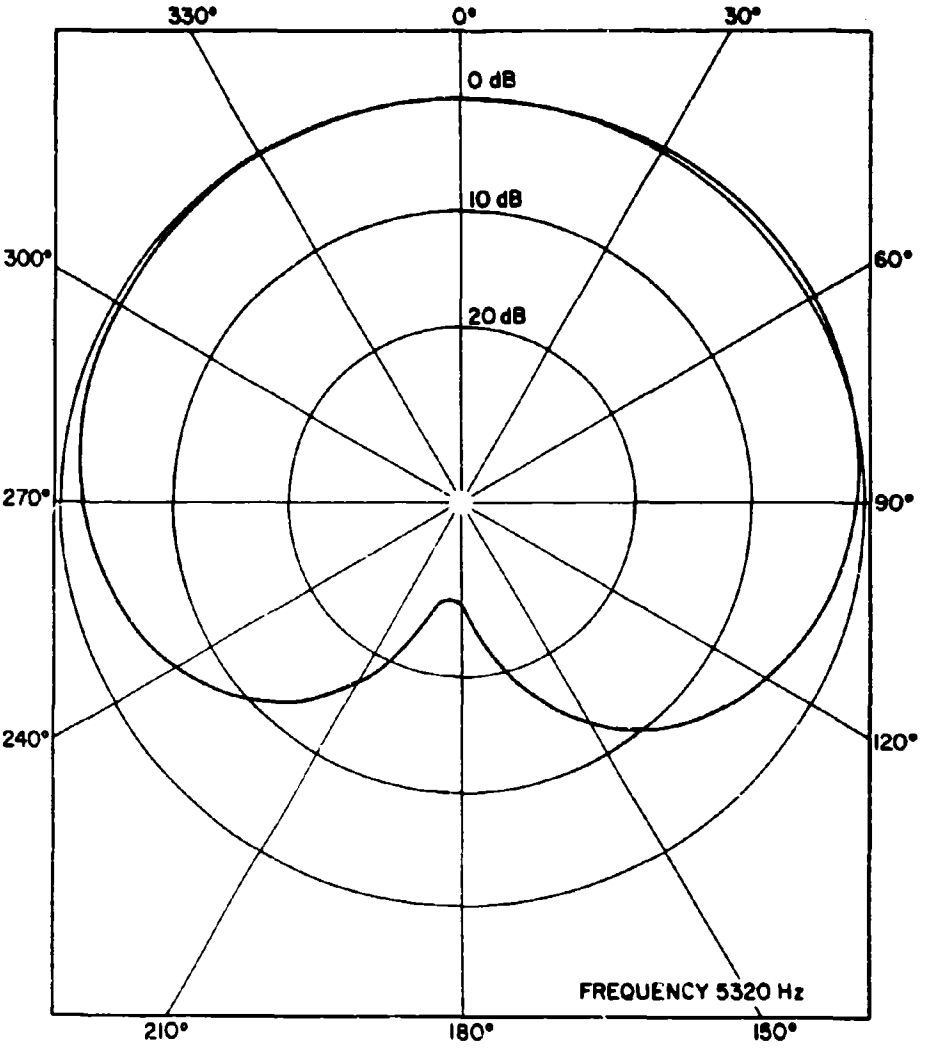

Figure 4.9. Directivity Pattern at 5320 Hz With the Specified Acoustic Phase-Shift Network Parameters (t = 0.028 cm)

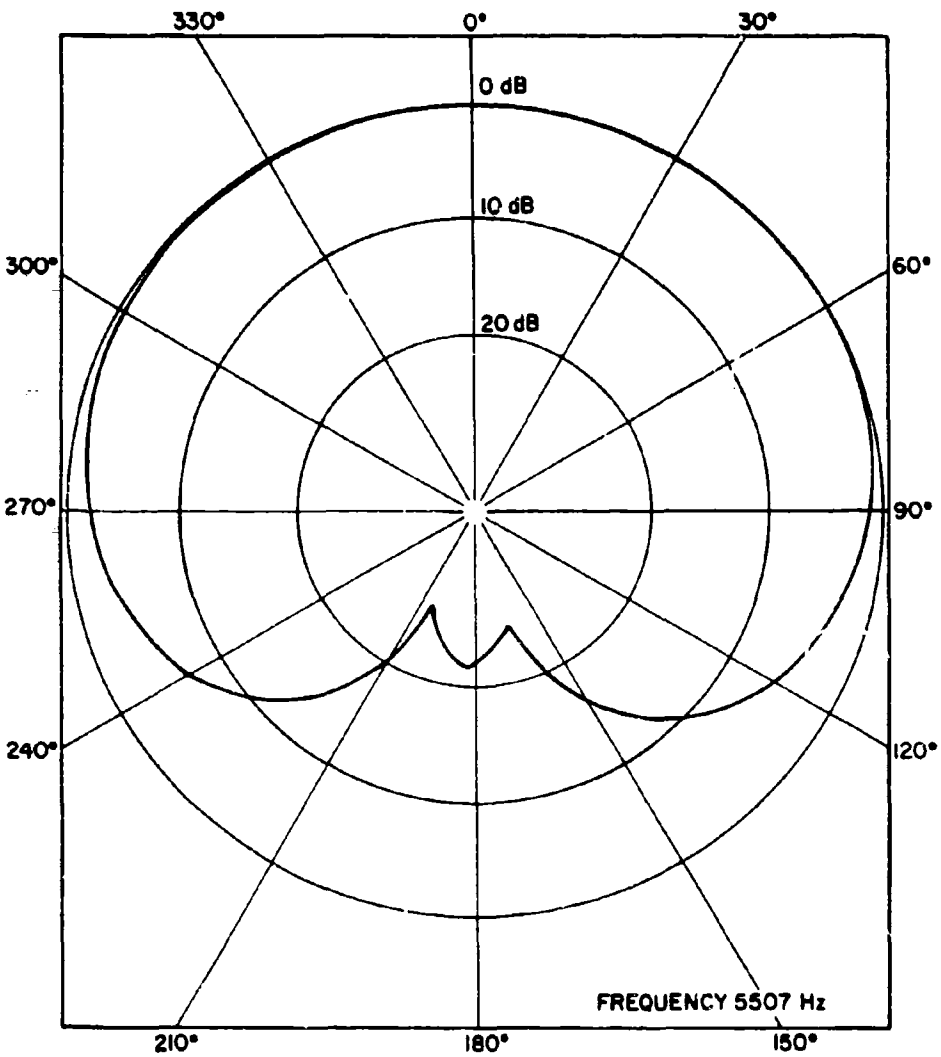

Figure 4.10. Directivity Pattern at 5507 Hz With the Specified Acoustic Phase-Shift Network Parameters (t = 0.028 cm)

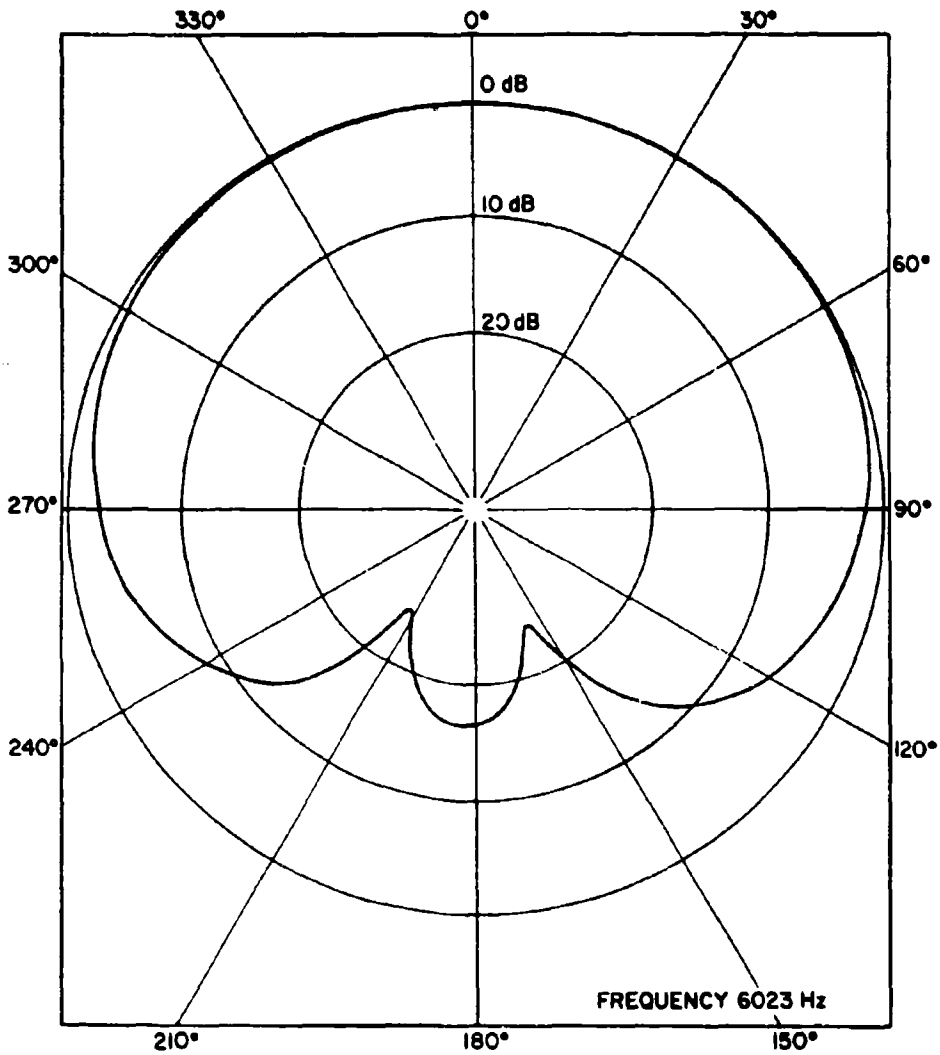

Figure 4.11. Directivity Pattern at 6023 Hz With the Specified Acoustic Phase-Shift Network Parameters (t = 0.028 cm)

A directivity pattern at 5000 Hz, as shown in Figure 4.17, was recorded at the Ordnance Research Laboratory's Black Moshannon Calibration Station, using a CW sound field instead of a pulsed field. The resulting plot of a unidirectional cardioid pattern with a front-to-back discrimination of 19 dB gave a reasonably good check on the data which was taken using pulsed techniques in the anechoic tank. Patterns at various other frequencies were also recorded using a CW sound field, showing very close agreement with the pulsed data.

Figure 4.18 shows the free-field voltage response (M_o) of the transducer model. The response, as shown, rose between 1000 Hz and 4000 Hz but was relatively flat ($M_o \approx -85$ dB) between 4000 Hz and 6000 Hz. However, the flat portion of the response occurred over a band where the unidirectional, cardioid action of the phase-shift network was optimum.

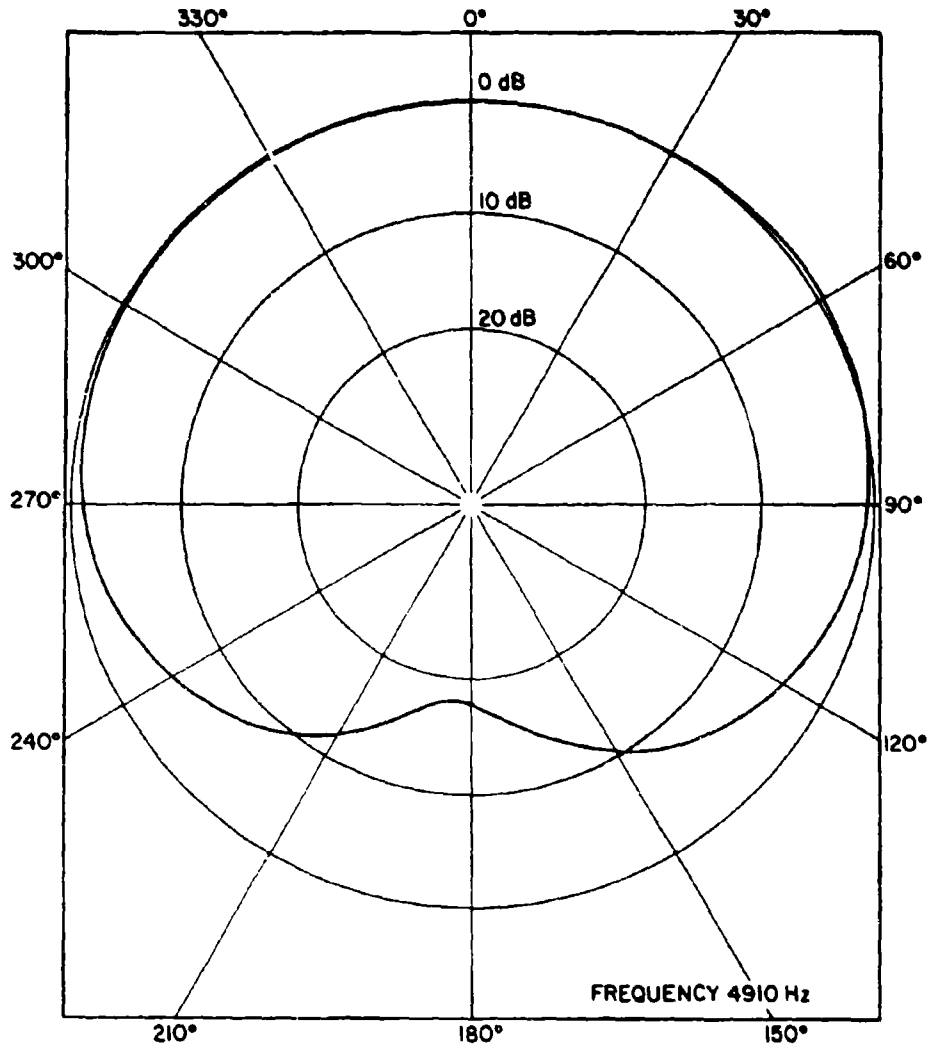

Figure 4.12. Directivity Pattern at 4910 Hz With the Specified Acoustic Phase-Shift Network Parameters (t = 0.028 cm)

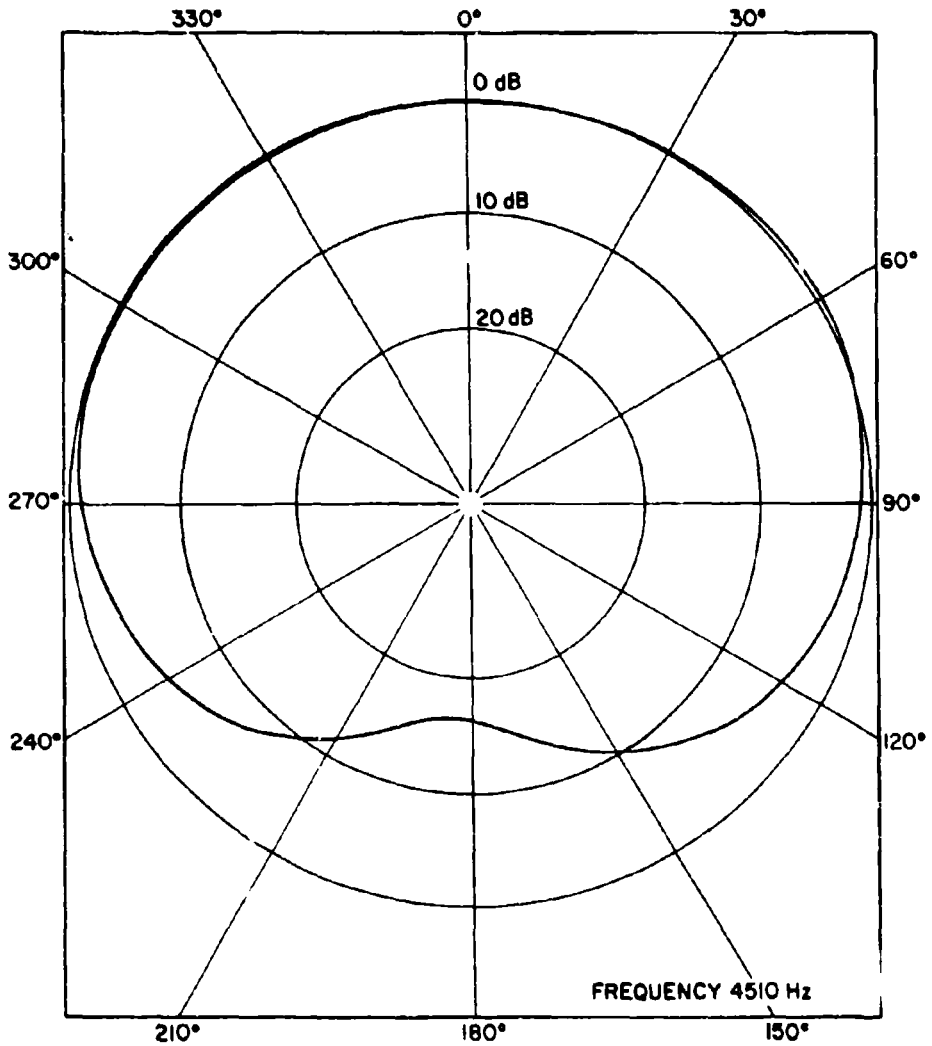

Figure 4.13. Directivity Pattern at 4510 Hz With the Specified Acoustic Phase-Shift Network Parameters (t = 0.028 cm)

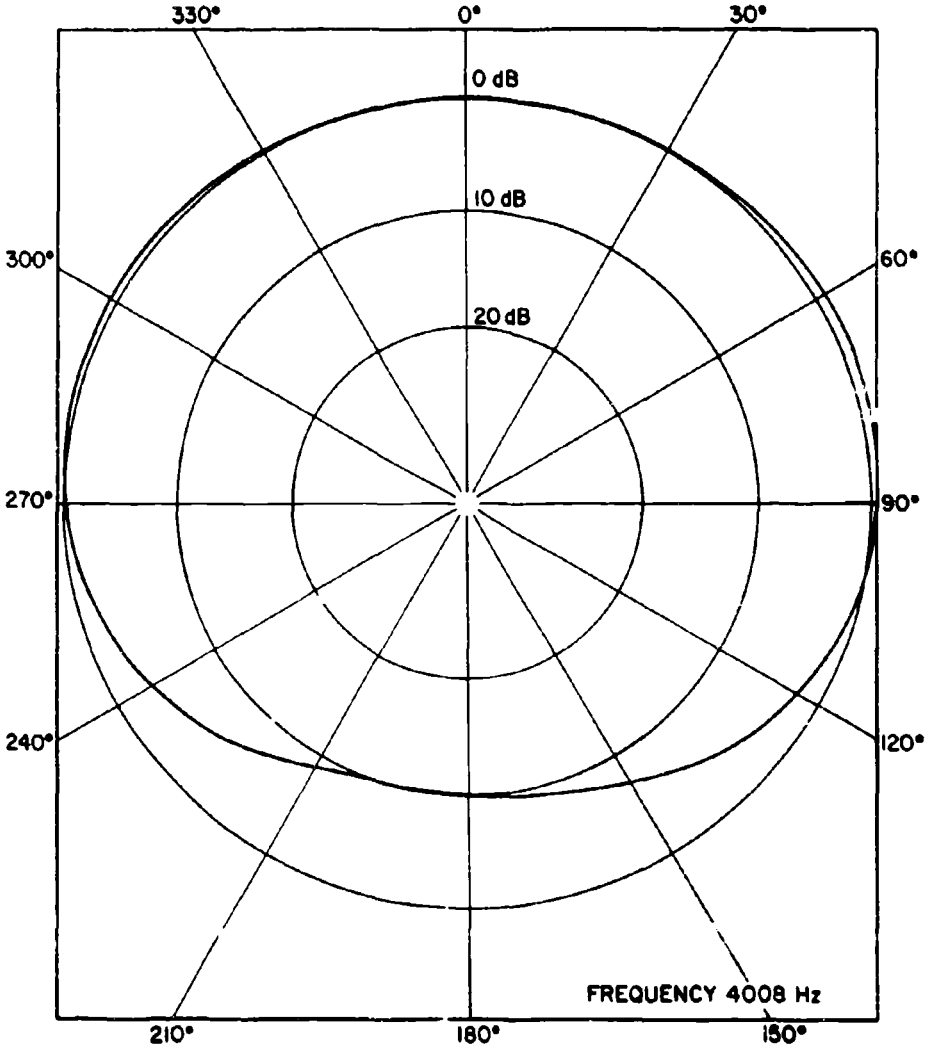

Figure 4.14. Directivity Pattern at 4008 Hz With the Specified Acoustic Phase-Shift Network Parameters (t = 0.028 cm)

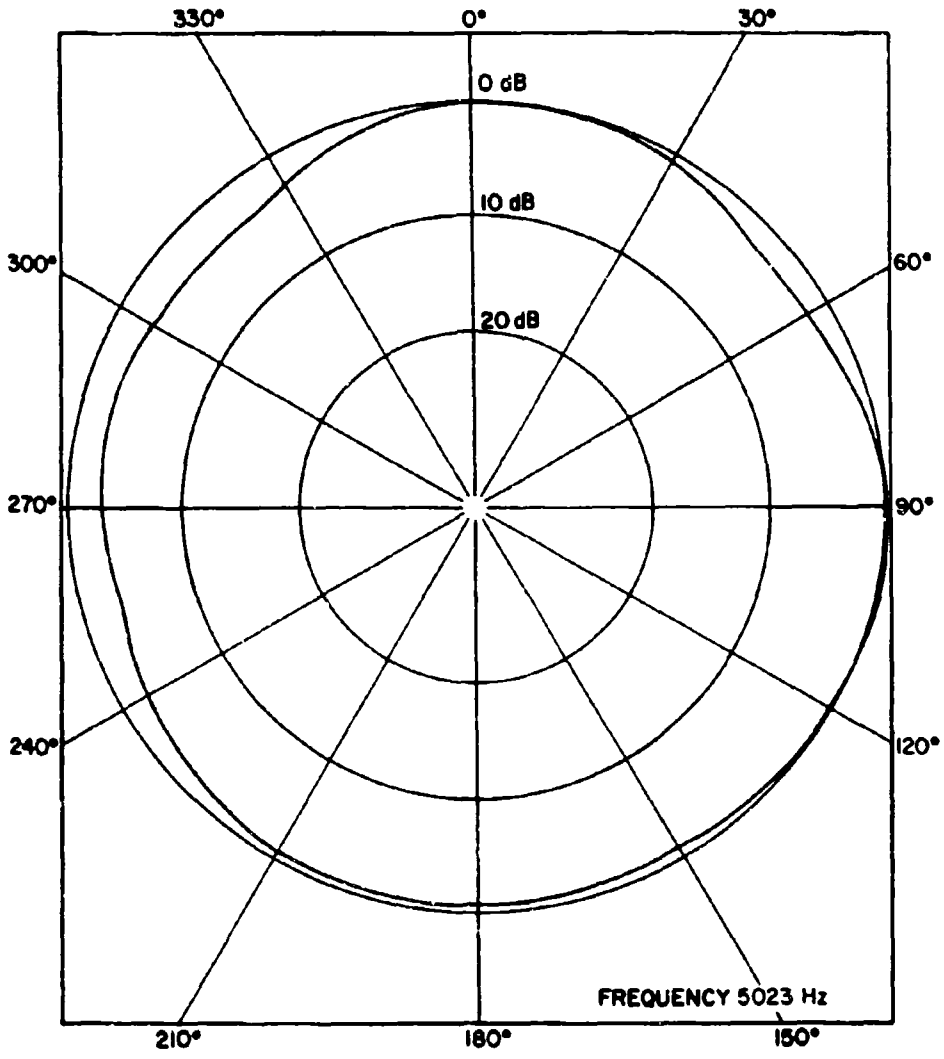

Figure 4.15. Directivity Pattern at 5023 Hz With the Specified Acoustic Phase-Shift Network Parameters (t = 0 cm)

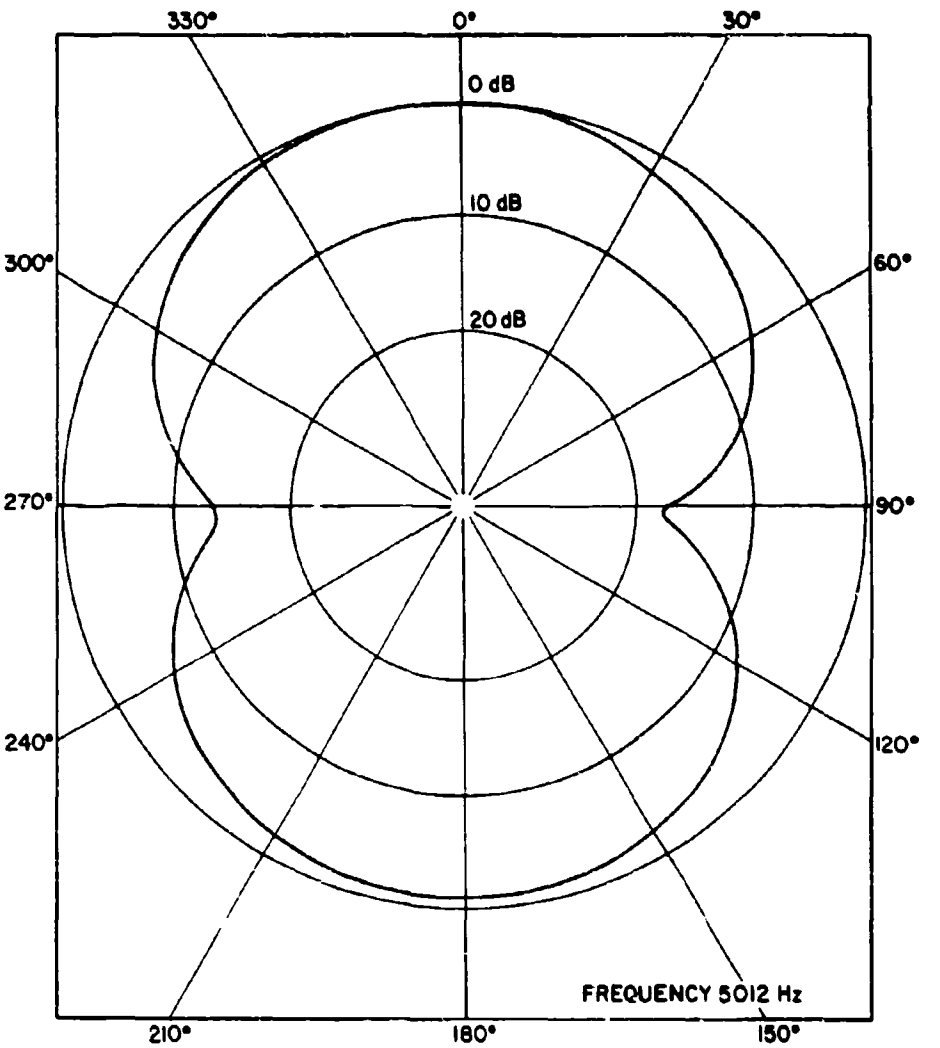

Figure 4.16. Directivity Pattern at 5012 Hz With the Specified Acoustic Phase-Shift Network Parameters (t = 0.254 cm)

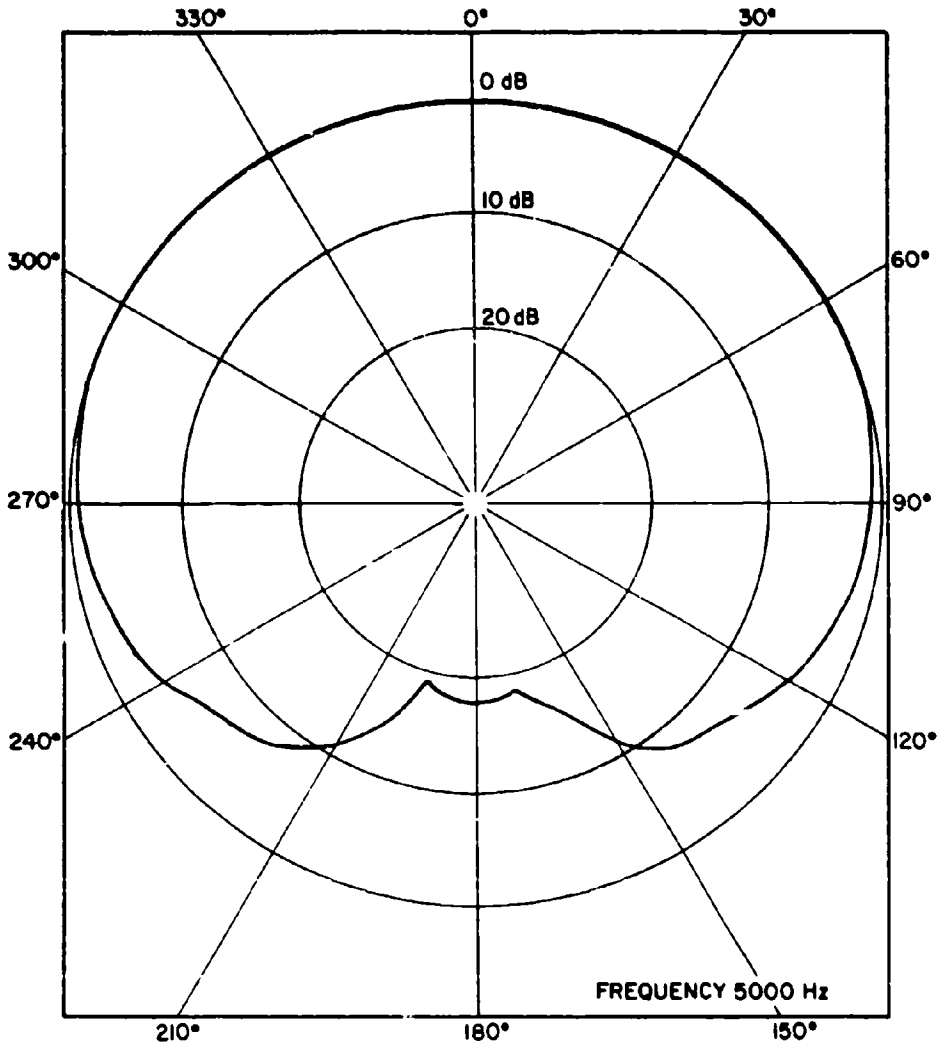

Figure 4.17. Directivity Pattern at 5000 Hz With the Specified Acoustic Phase-Shift Network Parameters Using a CW Sound Field

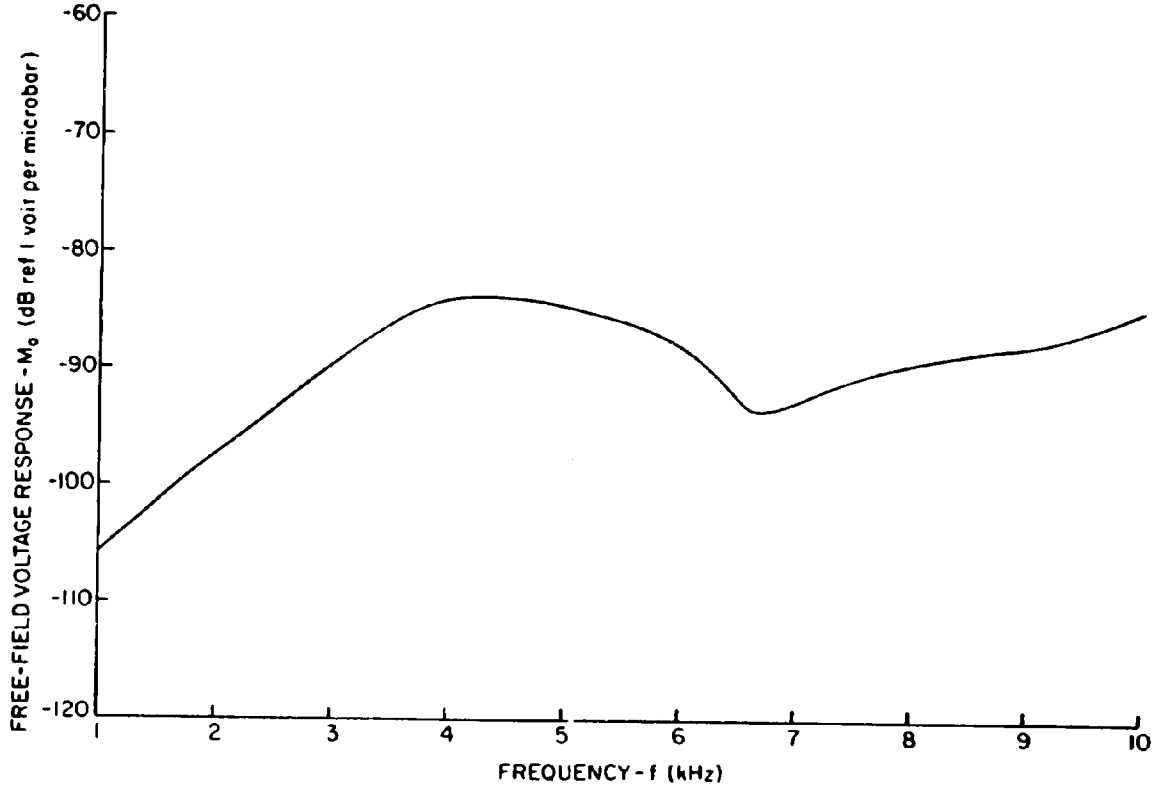

Figure 4.18. Free-Field Voltage Response (M_o) of the Transducer Model

CHAPTER V

SUMMARY AND CONCLUSION

5.1 Summary

The primary objective of this investigation was to develop a low frequency, underwater, transducer model which would exhibit a unidirectional, (cardioid) directivity response.

The solution chosen to accomplish this objective required that a liquid-filled, acoustic phase-shifted, trilaminar, pressure gradient transducer system be studied.

The investigation was initiated by the development of a theoretical model which was used as a design guide for the transducer model. Interrelationships between certain analogous acoustic phase-shift network parameters evolved from the development of the theoretical model. Consequently, considerable effort was directed at understanding these parameter interrelationships. Specifications were obtained from the acoustic circuit parameters which defined the acoustic phase-shift network requirements. These specifications defined the overall size and shape of the device. That is, the dimensions of the phase-shift network slot, (t,W,ℓ), the cavity volume, and the effective front-to-back distance were determined. Since the model had to be liquid-filled to satisfy the depth insensitive requirement, a thorough search was conducted of all

possible fluids which might be used in the rear cavity as the network "working fluid". A Dow-Corning 200 (200 cs) silicone oil with extremely stable physical characteristics when subjected to temperature and pressure changes was found to meet all of the network requirements. That is, the dynamic viscosity (μ_f), the density (ρ_f), the adiabatic bulk modulus (β_f), the inertness, and the overall stability of the fluid was found to comply with the restrictions that were imposed by the acoustic phase-shift network requirements.

A study of the pressure-gradient transducing element was made next, with a trilaminar, flexural, piezoceramic disk being selected for this purpose. Various types of element mounting arrangements were also tested with a circular, Vee-wedge, simple support selected as being optimum.

A transducer model, complete with a series of two high acoustic impedance, free-floating piston accumulators (to accommodate a change in fluid volume due to a change in temperature and pressure) and satisfying all of the network specifications was then constructed.

The transducer model's unidirectional performance was experimentally evaluated by recording the directivity response of the model in the following configurations:

a. Without the acoustic phase-shift network. (The model was simply a dipole receiver.)

b. With the acoustic phase-shift network; the working fluid used in the rear cavity being air.

c. With the acoustic phase-shift network; the working fluid used in the rear cavity being fresh water.

d. With the specified acoustic phase-shift network; the working fluid used in the rear cavity being the Dow-Corning 200 (200 cs) silicone oil.

No unidirectional performance was obtained with the model in any one of the first three configurations. Only predicted bidirectional and omnidirectional responses were recorded.

A unidirectional (cardioid) response was achieved consistently (between 4000 Hz and 6000 Hz) when the model was arranged as described in part d. Front-to-back discriminations ranging between 15 dB and 27 dB were recorded over the upper half of the frequency range (5000 Hz to 6000 Hz), while 10 dB to 15 dB discriminations were recorded over the lower half (4000 Hz to 5000 Hz) of the frequency range. The poorer discrimination at the lower frequencies is believed due to the fact that the rear cone was not sufficiently massive to preclude some significant shunting effect of the compliance C_3. A nominally flat free-field voltage response (M_o) of -85 ± 2 dB, reference 1 V/μbar, was also achieved over the frequency range of 4000 Hz to 6000 Hz.

5.2 Conclusions

The investigation has demonstrated that it is feasible to design and construct a single-element, pressure gradient transducer which is capable of providing a unidirectional, (cardioid) directivity response in an underwater environment. The preceding statement must be considered and qualified in the following manner:

1. A unidirectional, cardioid response with a reasonable front-to-back discrimination was achieved over the frequency range between 4000 Hz and 6000 Hz. The front-to-back discrimination, as in the case of the piezoelectric air microphone, exhibited a frequency dependence with a maximum discrimination of 27 dB occurring at 5300 Hz. Nevertheless, a reasonable directivity response with a reasonable front-to-back discrimination was achieved, utilizing the specified phase-shift network requirements, over the above-mentioned frequency range.

2. The specific definition of the problem stated that the performance of the transducer model should be insensitive to change in the ambient temperature. The principal component of the system which might affect the model's performance due to a temperature change would be the silicone oil working fluid. That is, the dynamic viscosity (μ_f), the density (ρ_f), and the adiabatic bulk modulus (β_f) of the oil could and actually did vary with a change in temperature. The acoustic network impedances Z_2 and Z_3, which depend on the values of these three characteristics, would also change. It might be expected that these changes in the parameters

of the acoustic phase-shift network would produce changes in the performance. However, it was experimentally observed that a change in temperature from 14°C to 22°C produced no measurable change in any characteristic of the directional pattern.

3. The specific definition of the problem indicated that the performance of the transducer model would be insensitive to a change in depth (hence pressure) since it was to be utilized in an underwater environment. Again, the principal component of the system which might affect the model's performance would be the silicone oil working fluid and for the same reasons as mentioned above. That is, ρ_f, μ_f, and β_f could vary with a change in hydrostatic pressure thus changing the acoustic network impedances Z_2 and Z_3. However, these characteristics change so little (see Section 3.1.2) that no significant change in the performance of the model is predicted over a 0 to 1000 psig pressure range. In fact, the increase in the effective compliance (C_3) with frequency from 4000 Hz to 6000 Hz due to the shunting effect of the rear cone mass ($M_{A\text{-CONE}}$) was approximately 40 percent. Although this large change in the effective compliance reduced the front-to-back discrimination of the model, it did not, by any means, completely eliminate it.

It should be noted that, although all of the data presented in this report were obtained with the model used as a hydrophone, nevertheless the model will serve as a sound projector because it is a reciprocal device. In fact, essentially identical directional patterns of the model were obtained when using it as a sound projector.

BIBLIOGRAPHY

1. Olson, H. F., U. S. Patent No. 1,885,001; 1932.

2. Olson, H. F., "A Unidirectional Ribbon Microphone," Journal of the Acoustical Society of America, Volume 3, p. 315; January 1932.

3. Weinberger, J., Olson, H. F., and Massa, F., "A Unidirectional Ribbon Microphone," Journal of the Acoustical Society of America, Volume 5, pp. 139-147; October 1933.

4. Baumzweiger (Bauer), B., U. S. Patent No. 2,184,247; 1939.

5. Baumzweiger (Bauer), B., U. S. Patent No. 2,237,298; 1941.

6. Bauer, B. B., "Uniphase Directional Microphones," Journal of the Acoustical Society of America, Volume 13, pp. 41-45; July 1941.

7. Bauer, B. B., Proceedings of the I.R.E.; May 1962.

8. Olson, H. F., Elements of Acoustical Engineering, D. Van Nostrand Company, Inc., New York, 1940; Chapter 4.

9. Bauer, B. B., "Equivalent Circuit Analysis of Mechano-Acoustic Structures," Transactions of the I.R.E.; June 1954.

10. Beranek, L. L., Acoustics, McGraw-Hill, Inc., New York, 1954; Chapter 3.

11. Woollett, R. S., "Theory of the Piezoelectric Flexural Disk Transducer with Applications to Underwater Sound," U. S. L. Research Report No. 490; December 1960.

12. Johnson, F. H., and Woollett, R. S., "A Flexural Ceramic Disk Transducer for Deep Water Operation," U.S.L. unpublished research report; 1963.

13. Marboe, R. F., and Farwell, R. W., "Absorption and Reflection Characteristics of a Water-Filled Anechoic Tank," Journal of the Acoustical Society of America, Volume 31; November 1959, (abstract only).

14. Dodge, R. A., and Thompson, M. J., Fluid Mechanics, McGraw-Hill, Inc., New York; 1937. Chapter 8.